

**Project ID/Title:** Synthesis of hybrid nanosorbent CaO incorporated with MgO-SiO<sub>2</sub> for enhancement CO<sub>2</sub> capture performance and cyclic stability

**Project Sponsor:** Research Initiative Grant Scheme (Publication) (P-RIGS)

**Author Name(s):** Farah Diana Mohd Daud, DR. Norshahida Binti Sarifuddin

**Department/Kulliyyah/Institute/Centre:** Engineering

**Abstract:**

A high magnitude of greenhouse gases, carbon dioxide (CO<sub>2</sub>) released into the air has been really alarming and contributing to climate disasters of global warming. Many studies reported that calcium oxide (CaO) is stoichiometrically and reversibly react with CO<sub>2</sub> used for CO<sub>2</sub> removal are not efficient for practical purpose due to sintering which suffer from structural instability, thus reduced capturing (adsorption) capacity and sorbent recyclability. The most important criterion to prevent the sintering and to increase the capturing capacity is to increase the surface area by manipulating CaO at the nano level with uniform distribution. The incorporation CaO with magnesium oxide and silica (MgO-SiO<sub>2</sub>) as hybrid nanosorbent would be beneficial because MgO and CaO alone have shown high capacity and affinity toward CO<sub>2</sub> at ambient (1 atm, 0-25°C), and flue gas (1 atm, 120°C) conditions, which after merging with SiO<sub>2</sub> can be substantially enlarged due to the high active surface area and well-developed porosity of the hybrid sorbents. Therefore, the ultimate aim of this work is to synthesis hybrid nanosorbent of CaO incorporated with MgO and SiO<sub>2</sub> via coprecipitation. The SiO<sub>2</sub> precursor will be produced using the natural source, silica sand through alkali fusion method. The CaO will be incorporated with MgO and SiO<sub>2</sub> at different ratio, synthesis temperature and time, catalyst concentration, type of solvent, and calcination temperature. The CO<sub>2</sub> capture of hybrid nanosorbent materials will be measured by using a thermogravimetric analyzer (TGA) at multiple cyclic of adsorption and desorption at different temperature. The synthesis nanosorbent is expected to have excellent sintering resistant (MgO) and structural stability (SiO<sub>2</sub>) which improved sufficiently cyclic adsorption/desorption operations. These findings will then benefit in capturing CO<sub>2</sub> whereby designated hybrid nanosorbent materials with optimum properties are reliable and can be fully utilized in the combustion flue gases, power plants, industrial processes and transport.

**Key words:** hybrid, nanosorbent, CaO, MgO-SiO<sub>2</sub>, CO<sub>2</sub>, capturing, multiple, cyclic

## Introduction:

Ca-based sorbents are a type of high temperature CO<sub>2</sub> sorbents with high theoretical sorption capacity of 17 mmol CO<sub>2</sub>/g sorbent and wide availability of precursor such as limestone and dolomite [1-3]. However, the adsorption/desorption reactions of CaO and CaCO<sub>3</sub> are far from complete or reversible. Rapid loss of CO<sub>2</sub> capacity over many adsorption/desorption cycles is always observed. It was found that the calcium conversion decreased from over 90% to a residual value 7–8% after prolonged cycles of adsorption/desorption (up to 500 cycles)[4]. This capacity decay of CO<sub>2</sub> capture of CaO over cycle has been mainly attributed to the severe sintering of CaCO<sub>3</sub> during desorption process [5-7]. The mechanism is believed to be as follows. The CaO particle is comprised of microporous grains of various sizes in crystals. During carbonation of CaO, CO<sub>2</sub> is transported through the spaces between the grains and then through the spaces between the crystals before it reaches the crystals and converts CaO crystals into CaCO<sub>3</sub> crystals. When the CaCO<sub>3</sub> crystals are regenerated subsequently at high temperature, which is normally higher than their sintering temperature (or Tammann temperature, ~533 °C), sintering occurs severely [8]. The sintering leads to the aggregation of calcium crystals/grains, which results in the less surface area of the produced CaO (i.e., the spaces between the crystals) available for the adsorption reaction in the next cycle. Thus, the rate as well as the extent of the gas–solid reaction, decays significantly, after each cycle of adsorption/desorption. According to the described mechanism, there are possibly two strategies to overcome sintering problem during many of adsorption/desorption : (i) breaking the sintered crystals again and therefore recovering the surface area (and performance) of the sorbent after sintering; and (ii) synthesizing sintering-resistant sorbent by separating CaO crystals/particles with inert particles to prevent sintering. Literature results show that both strategies would work; however, the first strategy would not be able to meet some other requirements on sorbent physical properties, while the second strategy would be able to meet all the requirements for practical applications. Among many metal oxides studied, CaO and MgO showed remarkably high CO<sub>2</sub> sorption at elevated conditions. Therefore, the incorporation CaO with MgO-SiO<sub>2</sub> as hybrid nanosorbent would be beneficial because MgO and CaO alone have shown high capacity and affinity toward CO<sub>2</sub> at ambient (1 atm, 0-25°C), and flue gas (1 atm, 120° C) conditions, which after merging with SiO<sub>2</sub> can be substantially enlarged due to the high active surface area and well-developed porosity of the hybrid sorbents. Therefore, the aim of this work are to find a method for production of hybrid nanosorbent without the problem of loss in capacity (less sintering effect) after multiple cyclic of adsorption/desorption. This is done by selecting appropriate synthesis technique and incorporating inert material such as MgO-SiO<sub>2</sub> into CaO sorbents via co-precipitation method. This method will generally allow control over the ratio of CaO to support (MgO-SiO<sub>2</sub>), they typically have ability to tailor the morphological properties of the CO<sub>2</sub> nanosorbent (surface area, pore volume, and pore size distribution). Furthermore, the MgO and SiO<sub>2</sub> have been selected due to

less sintering effect and ability to develop more stable porous structures of hybrid nanosorbent for better CO<sub>2</sub> capture performance and multiple cyclic stability.

### **Background:**

With the awareness of global warming and climate change, CO<sub>2</sub> captures have been extensively studied for reduction of its emission to atmosphere. Currently, the CO<sub>2</sub> emissions from anthropogenic sources reached 34.83 Gt in 2011 and accounted for 67% of total greenhouse gas emissions [9]. Therefore, various technologies are developing to replace fossil fuel such as nuclear energy, solar energy and biomass-based energy. Besides developing new energy technology, the CO<sub>2</sub> capture technologies parallel develop to reduce the emission of CO<sub>2</sub> which are becoming increased nowadays. A wide range of CO<sub>2</sub> capture technologies are recently exist such as chemical and physical absorption, chemical adsorption (zeolite, metal oxides, metal organic frameworks and carbon adsorbent, Pressures/vacuum pressure/temperatures swing approach), cryogenic separation/distillation, gas hydrated, chemical looping (metal oxides), membrane separation (inorganic, polymeric, hybrid membranes) and biological fixation [10-11]. The use of solid CO<sub>2</sub> adsorbents is generally considered as an alternative, potentially less-energy-intensive separation technology. Furthermore, this solid CO<sub>2</sub> adsorbents can be utilized from ambient temperature to 700 °C, yield less waste during cycling and the spent solid adsorbent can be disposed of without undue environmental precautions compared to liquid adsorbent so far [12]. A variety of solid physical adsorbents have been considered for CO<sub>2</sub> capture including microporous and mesoporous materials (carbon based sorbents such as activated carbon and carbon molecular sieves, zeolites, and chemically modified mesoporous materials), metal oxides, and hydrotalcite-like compounds [13]. These adsorbents can be classified into three types based on their sorption/ desorption temperatures: 1) low temperature adsorbents - 400°C (calcium based and alkali ceramic) respectively. However, these CO<sub>2</sub>-adsorbents suffer severely from textural degradation during the sorption/ desorption operations. Currently, these materials can only run several tens of cycles before any obvious degradation, and are still far from practical applications [14]. For instance the conversion of CaO decreased sharply from 70% in the first cycle to 20% in the eleventh cycle when tested in fluidized bed [14-15]. The deactivation primarily results from the formation of layer structured CaCO<sub>3</sub> surrounding the CaO which, once a certain thickness (e.g. 20 nm) is reached, severely hampers the diffusion of CO<sub>2</sub> to react with the inner core. It has also been reported that the adsorption capacity for CaO-based sorbents decays as a function of the sintering of CaO grain at high temperature and a certain loss in the porosity. When pores smaller than a critical value (e.g. 200 nm) are filled, the reaction gets much slower. Therefore, great efforts have to be made to enhance the cyclic stability of CaO-based sorbents. The use of natural and synthetic CaO-based sorbents has been investigated by

several researchers in recent years [16-17]. Since CaO sorbent alone suffers from rapid performance degradation over multiple cycles of carbonation and decarbonation, incorporation of inert and refractory support materials to CaO sorbents was studied to increase the stability. Hence, inert and refractory support materials with high Tammann temperature (TT) such as  $\text{Al}_2\text{O}_3$ ,  $\text{MgO}$ ,  $\text{SiO}_2$ ,  $\text{ZrO}_2$ ,  $\text{Y}_2\text{O}_3$ ,  $\text{MnCO}_3$ , and  $\text{La}_2\text{O}_3$ , were incorporated into CaO sorbents, and thus achieved more stable hybrid-structures and higher 40 cyclic  $\text{CO}_2$  uptakes [18]. Yang et al. used a natural CaO magnesium oxide ( $\text{MgO}$ ) sorbent and showed that it could absorb up to 10.2 moles of  $\text{CO}_2$  per kg of sorbent ( $\text{molCO}_2/\text{kgsorbent}$ ) at  $650^\circ\text{C}$  in the presence of water ( $\text{H}_2\text{O}$ ) and nitrogen gas ( $\text{N}_2\text{O}$ ) [11]. The core/shell sorbents were prepared by Mahinpey et al. with a protective porous shell using the mesoporous silica and titania layers [18]. These authors concluded that, the sintering issues of a CaO-based material have not been completely addressed in this research. Further study on sintering is required to understand this phenomenon and to determine its resolution by using novel materials as binders and promoters. Therefore, in this research, the CaO will be incorporated with  $\text{MgO-SiO}_2$  as hybrid nanosorbent to overcome and resolve this issue for excellent  $\text{CO}_2$  capture at multiple cyclic of adsorption and desorption.

### **Objectives:**

The main aim of this research is to develop hybrid nanosorbent for  $\text{CO}_2$  adsorption without any drastic decay in adsorption capacity over multiple cycles. Therefore the objectives of this work are as follows:

1. To synthesize CaO incorporated with  $\text{MgO}$  and  $\text{SiO}_2$  as hybrid nanosorbent via co-precipitation for good structure stability and less sintering effect.
2. To characterize of hybrid sorbent of CaO incorporated with  $\text{MgO-SiO}_2$
3. To evaluate  $\text{CO}_2$  capture capacity and efficiency of synthesized hybrid nanosorbent by thermal gravimetric analysis (TGA) at multiple cyclic  $\text{CO}_2$  adsorption/desorption

### **Methodology:**

#### **Phase 1: Synthesis of hybrid nanosorbent of CaO incorporated with $\text{MgO}$ and $\text{SiO}_2$**

##### **Method 1:**

The CaO-based  $\text{MgO}$  adsorbent synthesis via new and facile method which is two-step method. Magnesium nitrate (29.66 g) and calcium acetate (8.3 g) is mixed in 10 ml of distilled water with constant stirring. Then, ethanol was added dropwise to the mixture at room temperature. After the mixture had become gel, the sample proceeded with calcination process at  $550^\circ\text{C}$  and  $650^\circ\text{C}$ . The prepared CaO- $\text{MgO}$  sorbent is then characterized by using Scanning Electron Microscopy (SEM) and X-Ray Diffraction (XRD) to observe the surface morphology and the crystallinity phase of the sample.

Identification of functional groups of producing Ca-based MgO adsorbent was confirmed using fourier transfer infrared spectroscopy (FTIR).

### **Method 2:**

The rice husk was from Muar, Johor. Other materials used are the distilled water, HCl (R&M chemical of 37%), H<sub>2</sub>SO<sub>4</sub>(Sigma-Aldrich, 99%) and NaOH (Merck). Nanosilica was extracted from RHA via precipitation method, starting with washing the rice husk with distilled water. Then, the washed rice husk has been sun dried for 12 hours, followed by burning of the rice husk at a temperature of 800 °C for 3 hours. After cooling, RHA was obtained. The RHA was subjected to acid leaching using 1 M of HCl and thermal treated inside the furnace set up at 650 °C for 3 hours. The dried RHA were then refluxed at 70 °C with three different concentrations of NaOH solution which are 0.5 M, 1.5 M, and 2.5 M, while being stirred for 4 hours. After the reaction, sodium silicate was formed. After completing this step, concentrated H<sub>2</sub>SO<sub>4</sub> was then added into them drop by drop with constant stirring until the pH of the mixture became 8. Next, the precipitate was washed by using distilled water until the pH is equal to 7. Followed by the filtering process using centrifuge machine in order to remove all the water content. The obtained residue were heated in an oven at fixed concentration of NaOH with three different temperature and different heating time which are 50 °C, 80 °C and 100 °C for 16 hours, 32 hours and 48 hours. Finally, the dried nanosilica powder that were obtained and characterizations for the final samples have been done.

### **Method 3**

Acetone, ethanol and deionized water were used in preparation of CaO-SiO<sub>2</sub> adsorbents. Calcium carbonate (CaCO<sub>3</sub>) powder and rice husk ash (RHA) from R&M Chemicals were mixed according to the specific weight ratio of CaO-SiO<sub>2</sub> adsorbent for each composition. CC:RHA ratio Mass (g) CaCO<sub>3</sub> powder RHA 90:10 9 1 80:20 8 2 70:30 7 3 In a cleaned mortar, CaCO<sub>3</sub> powder and RHA were physically mixed together and grinded at different grinding time (20, 30 and 40 minutes) with addition of acetone to smooth the mixing process. Next, the mixture undergoes calcination process in a muffle furnace at 700 °C with heating rate of 10 °C/min and holding time of 2 hours.

### **Method 4**

Calcium hydroxide from R&M Chemical Sdn. Bhd. was selected as the calcium precursor. The rice husk ash (RHA) as the biotemplate material was obtained from MARDI Perlis. Initially, RHA is oven-dried at 70 °C overnight to eliminate moisture. Then, the fine powder of RHA is obtained by ball milling process at 200 rpm for 1 hour. Finally, the ball milled RHA was sieved at the size range of 50 µm to 90 µm. Next, Ca(OH)<sub>2</sub> and RHA powders were weighed according to two different ratios Ca(OH)<sub>2</sub>: RHA ( 80:20 and 70: 30). At first, the weighed materials were vigorously mixed in a

granulator machine at 73 rpm speed for 10 minutes. Then, the mixture undergoes granulation process at the speed of 1700 rpm and simultaneously wetted by spraying 300 ml of deionized water. After the granulation process, the  $\text{Ca}(\text{OH})_2$ -RHA pellet was obtained in spherical shape and randomly in size. Lastly, the  $\text{CaO-SiO}_2$  pellets were obtained after calcination process in furnace at  $750^\circ\text{C}$

### **Phase 2: Characterization of hybrid sorbent of CaO incorporated with MgO-SiO<sub>2</sub>**

The hybrid sorbent of CaO incorporated with  $\text{MgO-SiO}_2$  will be characterized using X-ray diffraction (XRD) analysis, FESEM for morphological analysis, and Brunauer-emmet-Teller (BET) method through surface area analyzer.

### **Phase 3: CO<sub>2</sub> sorbent performances and multiple cycle capture via TGA method**

The CO<sub>2</sub> capture (adsorption and desorption performance) of the hybrid sorbents of CaO incorporated with  $\text{MgO-SiO}_2$  materials will be measured by using a thermogravimetric analyzer (TGA). The CO<sub>2</sub> capture capacity of the sorbents will be determined by measuring the mass uptake of the sample when exposed to pure CO<sub>2</sub>. Capacity was expressed as mass percentage of dry adsorbent. In a typical measurement procedure, the hybrid sorbent will be first activated under N<sub>2</sub> flow gas to remove any small molecules physically adsorbed. After the temperature was reduced, the samples will be allowed to adsorb CO<sub>2</sub> by replacing the N<sub>2</sub> gas flow by CO<sub>2</sub>. This process will be continued to measure CO<sub>2</sub> uptake of the sample. The adsorption/desorption cycling performance of the samples will also be measured at different temperatures. The samples after adsorption of CO<sub>2</sub> will be heated in a nitrogen atmosphere and cooled down, to allow adsorption of CO<sub>2</sub> again. This process will be repeated for multiple cyclic to evaluate any changes in CO<sub>2</sub> uptake.

## **Finding- Result and Discussion:**

### **Method 1**

Scanning Electron Microscope (SEM) is used in order to study surface morphology of the sorbents. The morphology of CaO-MgO sorbent calcined at  $550^\circ\text{C}$  shown in Fig. 1. Three magnifications are used in this characterization which are 500X, 2000X and 5000X which shown in Figure 4.1(a), Fig.1(b) and Fig. 1(c) respectively. It can be clearly observed that it has more porosity. For Fig. 2, SEM images shown are for CaO-MgO calcined at  $650^\circ\text{C}$  with 500X, 2000X and 5000X magnifications in Fig. 2(a), Fig. 2(b) and Fig. 2(c) respectively. From the observation, it is clear that this sample has less porosity compared to Fig. 1. However, both samples have irregular granules structures.

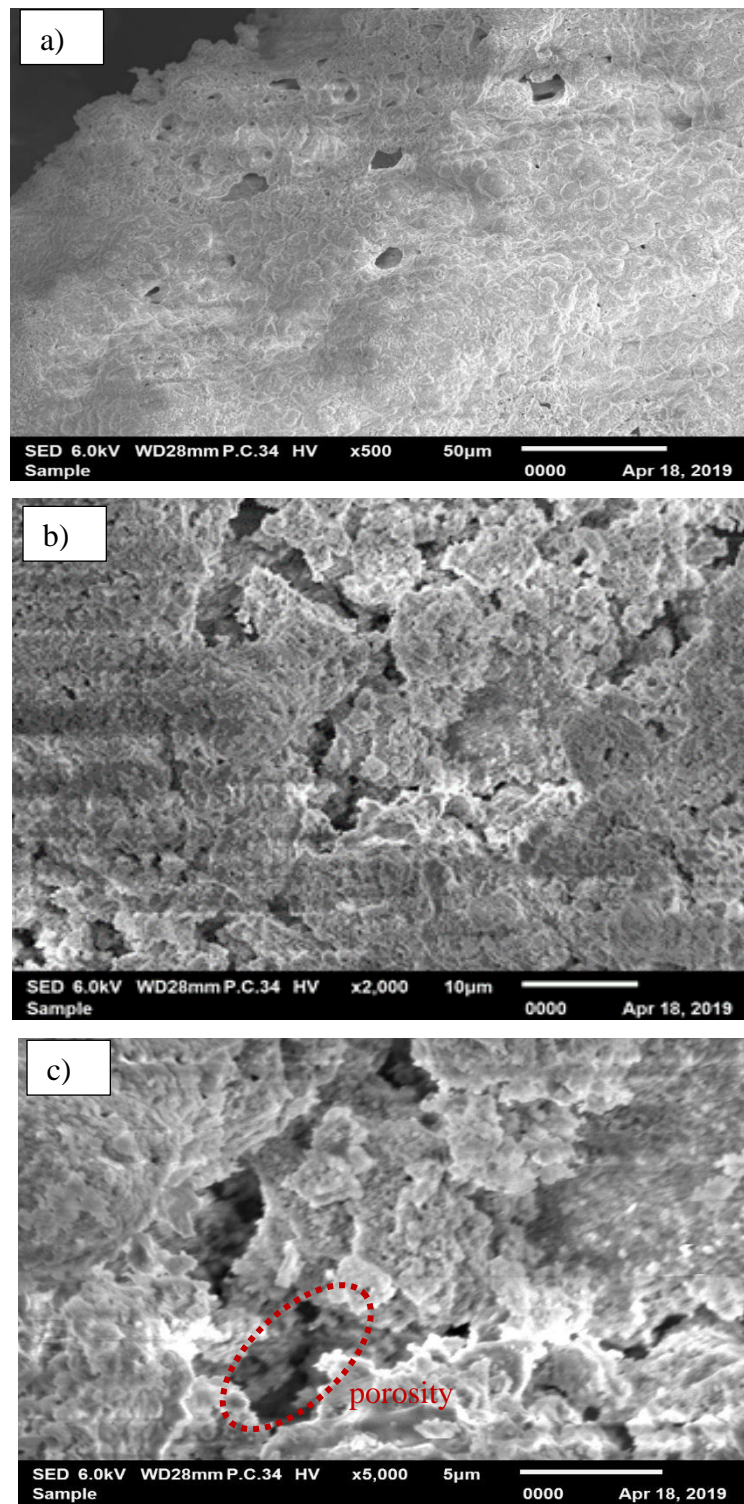


Fig. 1: SEM images for 0.2CaO-MgO calcined at 550°C at magnification:

(a) 500X, (b) 2000X and (c) 5000X

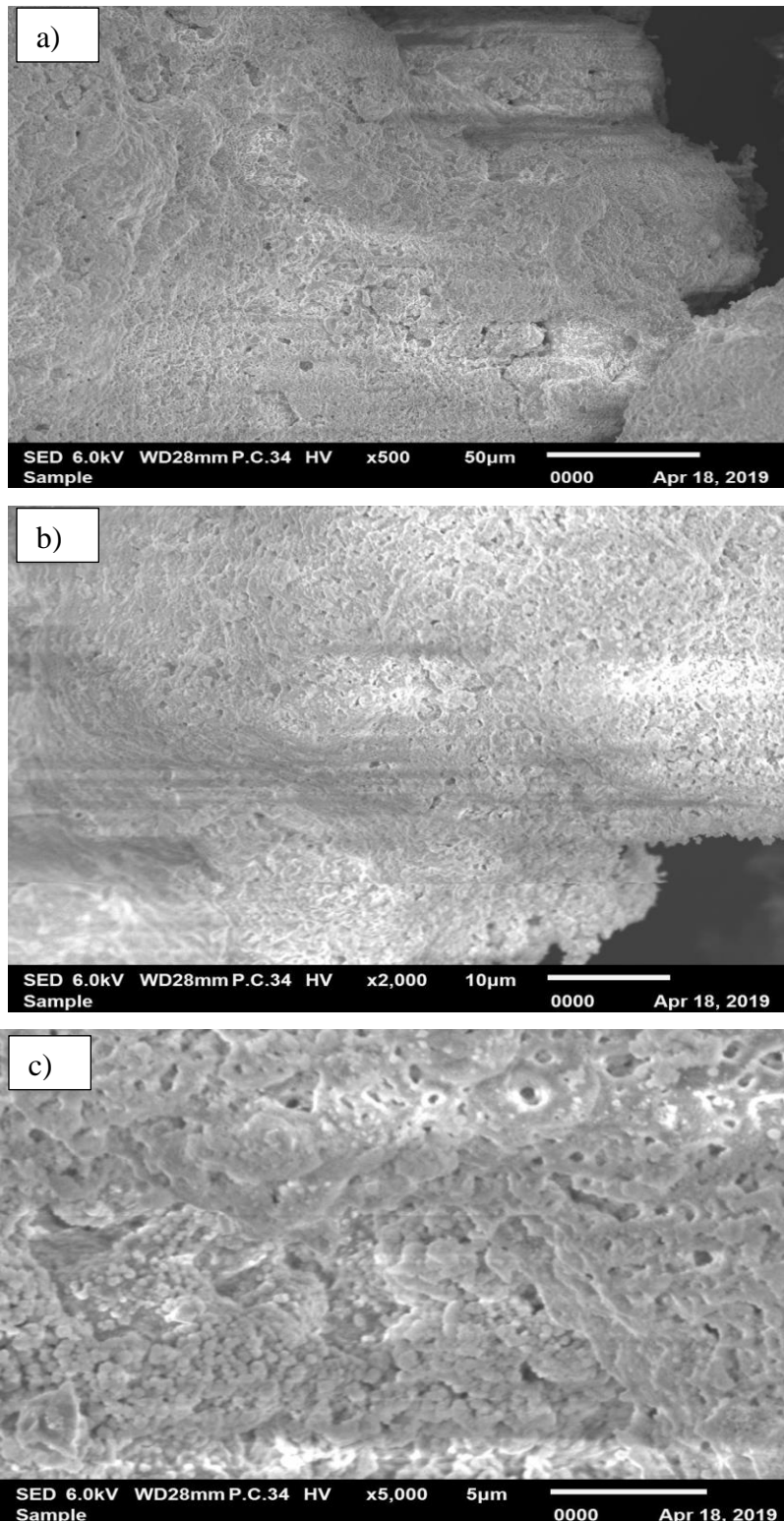


Fig. 2: SEM images for 0.2CaO-MgO calcined at 650°C at magnification:  
(a) 500X, (b) 2000X and (c) 5000X



The CaO-MgO sorbent are tested with XRD in order to identify the phase and also the crystal structure. Fig. 3 illustrated XRD pattern of CaO-MgO sorbent that had been calcined at 550°C while Fig. 4 illustrated XRD pattern of CaO-MgO sorbent calcined at 650°C. Both figures showed the existence of MgO and CaO mixed with CaCO<sub>3</sub> for both samples. In Fig. 3, the peaks at 2 $\theta$  at 43.04° and 62.35° were the peak for MgO (periclase) whereas at 23.2°, 36.15°, 39.55°, 47.6°, 57.55°, 64.75°, 74.9°, 78.65° and 29.53° which has the highest peak illustrated the existence of CaO mixed with CaCO<sub>3</sub> (calcite). XRD pattern in Fig. 4 is similar with the Fig. 3 with a slightly different 2 $\theta$ . The peaks at 2 $\theta$  at 43.05° and 62.35° showed the existence of MgO while the peaks at 23.25°, 36.25°, 39.65°, 47.5°, 57.75°, 78.7° and 29.55° which has the highest peak intensity showed the existence of CaO mixed with CaCO<sub>3</sub>. It is clearly observed that the peak intensities of Ca-based MgO calcined at 650°C are higher compared to Ca-based MgO calcined at 550°C which indicates it has good crystallinity.

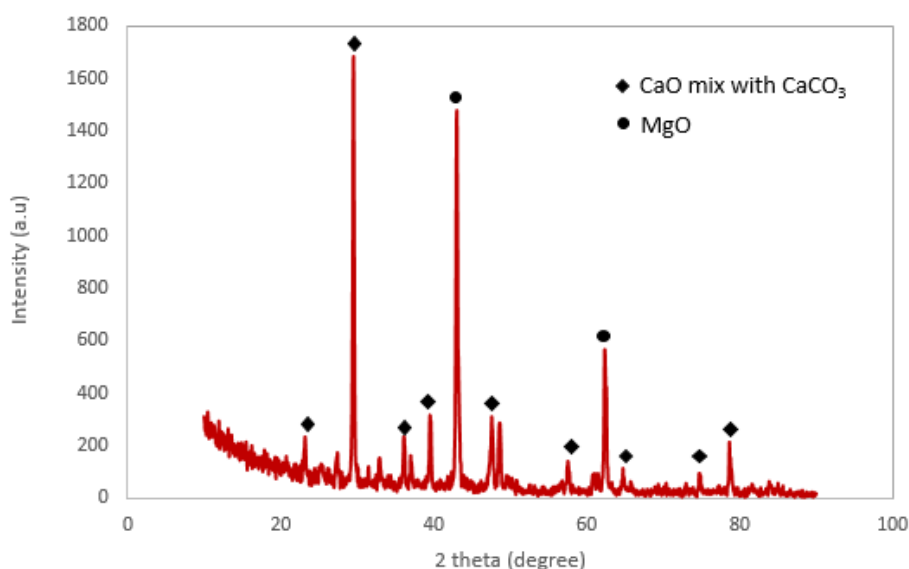


Fig. 3: XRD Pattern of CaO-MgO calcined at 550°C

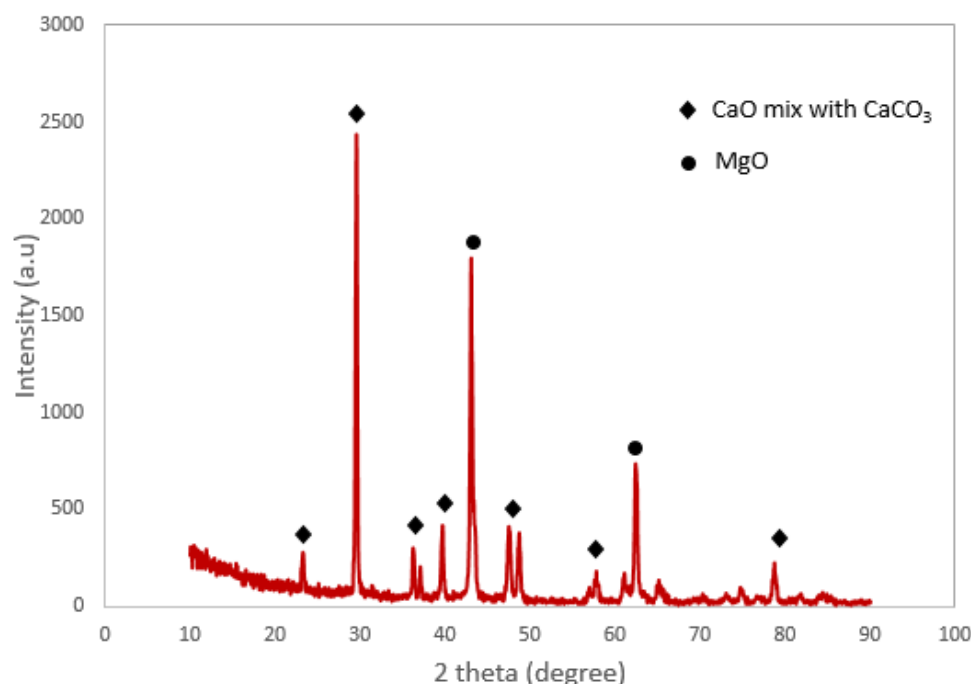


Fig. 4: XRD Pattern of CaO-MgO calcined at 650°C

The FTIR analysis of the synthesized Ca-based MgO adsorbent for various calcination temperature 550 °C and 650°C are shown in Fig. 5 and Fig. 6. The relatively low intensity band at 3628 cm<sup>-1</sup> corresponded to O—H bond matching with a low concentration of Ca(OH)<sub>2</sub> in the Fig.5. The hydroxide is a remaining component of the carbonation process. The minor bands at 2880 cm<sup>-1</sup> (Fig. 5) and 2878 cm<sup>-1</sup>(Fig.6) corresponds to C=O from carbonate ion. The intense and wide band at 1410 cm<sup>-1</sup> corresponds to C—O bonds from carbonate. The band at 874 cm<sup>-1</sup> corresponds to Ca—O bonds. The characteristic vibrational frequency of Mg=O bond at 655cm<sup>-1</sup> and 658 cm<sup>-1</sup>is demonstrated in Fig. 5 and Fig. 6. The spectra peak at around 433 to 769 cm<sup>-1</sup> is assigned to the metal—oxygen bending vibration.

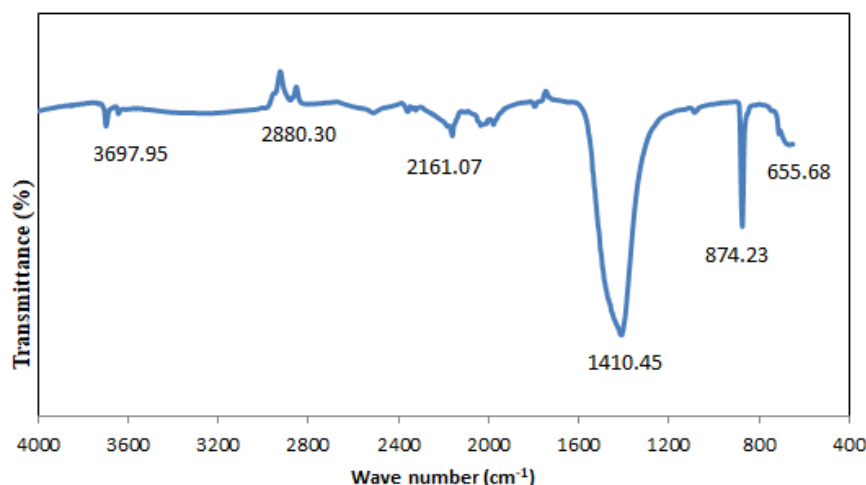


Fig. 5: FTIR spectra of CaO-MgO calcined at 550°C

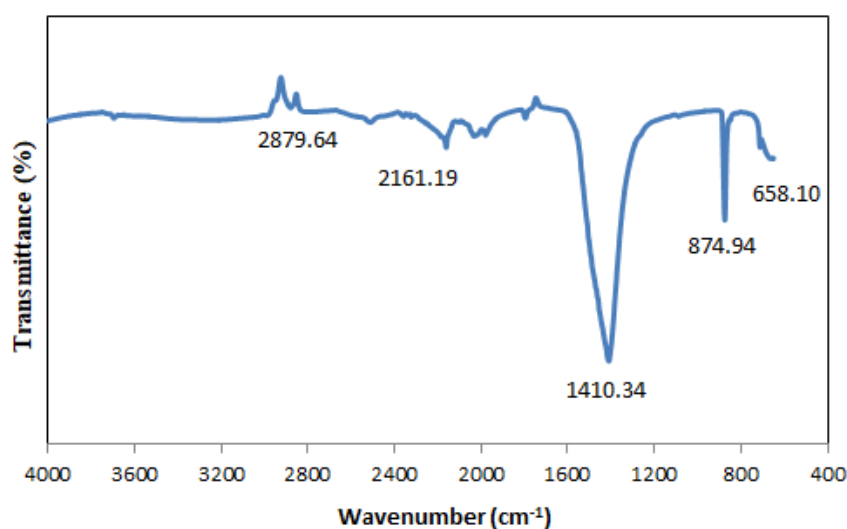


Fig. 6: FTIR spectra of CaO-MgO calcined at 650°C

## Method 2

Table 1, Table 2 and Table 3 summarized the composition of elements in all samples. During synthesis, acid leaching was done again on the samples with higher concentration of acid which is 6 M of HCl before the process of nanosilica extraction by adding NaOH and followed by H<sub>2</sub>SO<sub>4</sub>, which aims to completely remove the remaining inorganic oxides inside the RHA. Based on results tabulated, it can be seen that all of the other oxides have been successfully removed, which leads to higher purity of silica. However, it can be found that sodium and iron are exist. This may be due to the effect of addition of NaOH and the samples were not washed properly until all of the sodium content were removed.

Table 1: Percentage of elements for samples with varied NaOH concentration

Concentration of NaOH (M)	Percentage of Elements (%)		
	SiO <sub>2</sub>	Na	Fe
0.5	76.10	0.25	0.30
1.5	83.30	0.11	0.26
2.5	100.00	N/A	N/A

Table 2: Percentage of elements for samples with varied heating time

Heating time (hours)	Percentage of Elements (%)		
	SiO <sub>2</sub>	Na	Fe
16	68.00	0.50	0.40
32	77.96	4.83	11.92
48	100.00	N/A	N/A

Table 3: Percentage of elements for samples with varied heating temperature.

Heating temperature (°C)	Percentage of Elements (%)		
	SiO <sub>2</sub>	Na	Fe
50	100.00	N/A	N/A
80	79.80	0.12	0.31
100	97.40	0.27	0.36

For the samples with varied concentration of NaOH from 0.5 M, 1.5 M and 2.5 M heated for 48 hours and 50°C, the elemental percentage is shown in Table 1. It is clear that sample treated with 2.5 M NaOH produced the highest silica content with 100% purity. It undergoes the addition of highest concentration of NaOH as compared to the other two samples. This means that higher concentration of NaOH will cause higher dissolution or suspension of silica from the other elements or contaminants exist inside the RHA. The impurities are not dissolved inside the product and were removed during washing. The act of NaOH concentration as a cleaning agent, which can remove the other impurities, leading to higher purity of silica inside the final product. Thus, in this project, the highest concentration of NaOH which is 2.5 M is the best concentration to yield highest purity of silica.

The sample treated with 2.5M NaOH produced the highest silica content with 100% purity. It undergoes the addition of highest concentration of NaOH as compared to the other two samples. This means that higher concentration of NaOH will cause higher dissolution or suspension of silica from the other elements or contaminants exist inside the RHA. The impurities are not dissolved inside the product and were removed during washing [7]. By observing the XRD patterns for samples treated with 0.5 M, 1.5 M and 2.5 M NaOH concentrations at fixed heating time of 48 hours and temperature of 50°C as illustrated in Fig. 1, it can be seen that the silica particles are all in amorphous form due to the broad peaks that are observed at  $2\theta$  equals to 23°. In addition, although the silica phase is dominantly amorphous for sample treated at 2.5 M, it also provides intense peaks at  $2\theta$  equals to 19°, 28°, 29°, 32°, 34°, 38°, 48° and 54°. This is due to the formation of tridymite, which is the stable state of silica that can be found when using this particular concentration [5]. Meanwhile for samples with varied heating time for 16 hours, 32 hours and 48 hours at fixed temperature of 50°C and treated with 2.5 M NaOH as in Fig. 2, the broad peaks at  $2\theta$  equals to 22.70° confirm the amorphous state of silica. There is no significant difference between the curves for these three samples. This may be due to the fixed concentration of NaOH solubilized only amorphous state of silica, which is technically precipitated. Hence, it can be said that heating time does not affect the phase of silica present [8].

Whereas the XRD patterns for samples that are treated with varied heating temperature at 50°C, 80°C and 100°C, for fixed 48 hours fixed 2.5 M NaOH as illustrated in Fig.3 shows that the broad peaks are at  $2\theta$  equals to 22.10°. The absence of sharp peaks indicates that the phase of silica particles inside these samples are all in amorphous state. Therefore, silica particles maintain their phase during pre-synthesis and post-synthesis process [9].

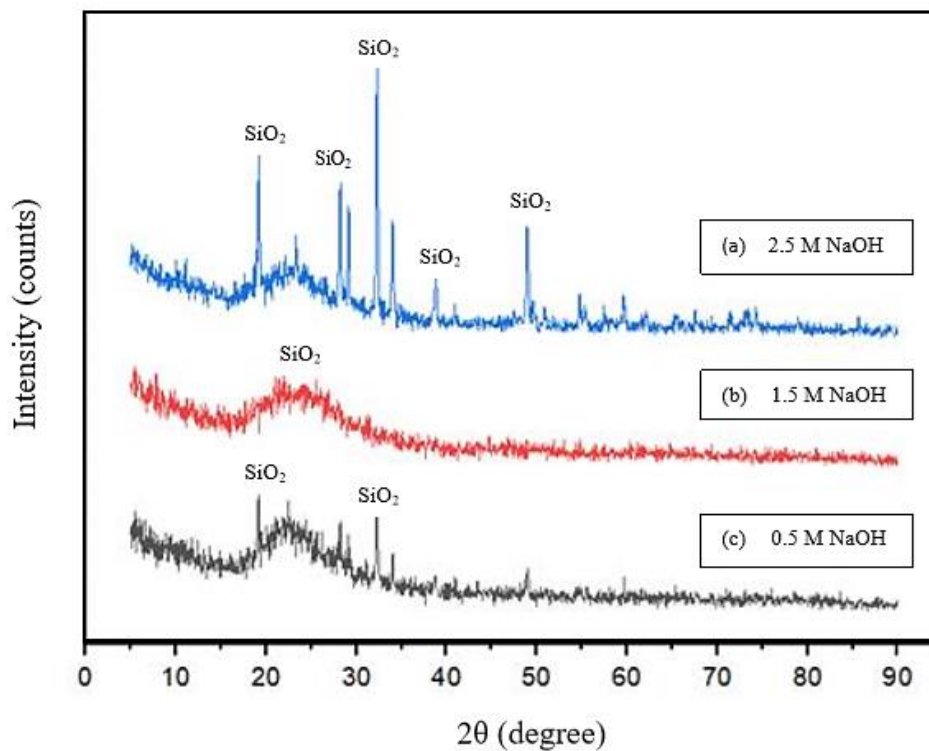


Fig. 1: XRD patterns for samples treated with 0.5 M, 1.5 M and 2.5 M NaOH

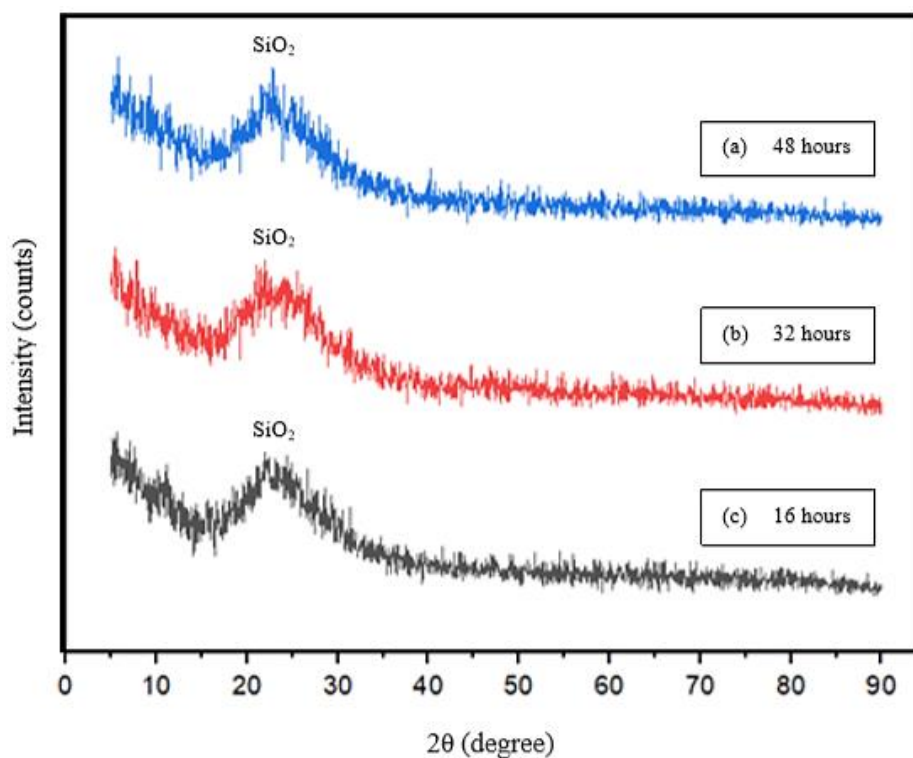


Fig. 2: XRD patterns for samples heated for 16 hours, 32 hours and 48 hours

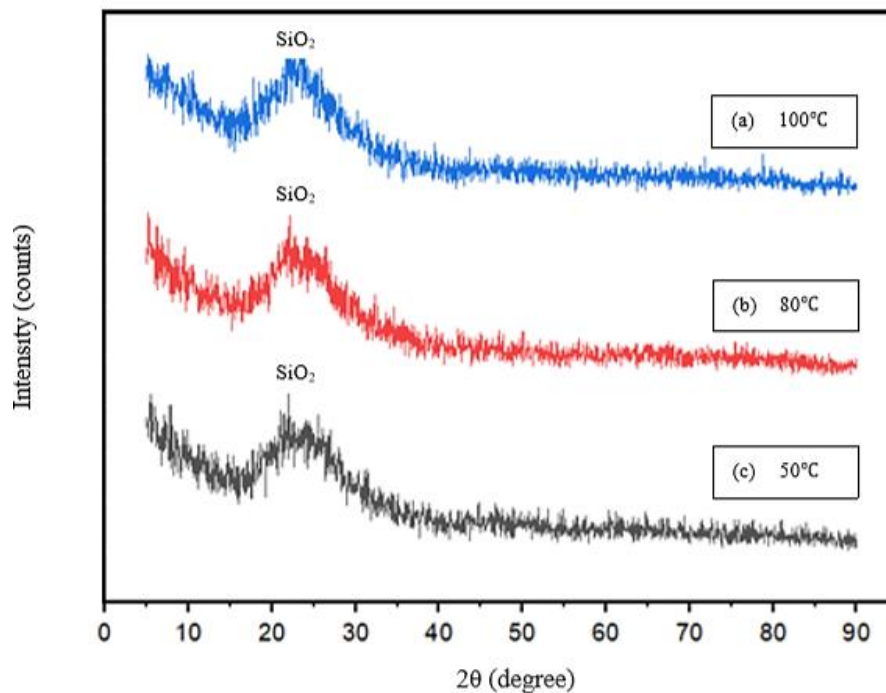


Fig. 3: XRD patterns for samples treated at 50°C, 80°C and 100°C

Fig. 4 illustrates the SEM images at magnifications of 250X and 10,000X for samples treated with varied NaOH concentrations ranging from 0.5 M, 1.5 M and 2.5 M at fixed heating time of 48 hours and temperature of 50°C. It is clear that agglomerated silica particles are found. This is caused by the non-conductive behaviour of silica which fasten the charges accumulation on the surface of the powder even after sputtering with Palladium. On the other hand, the uniformity of agglomerated spherical shape of silica particles can be seen improving with increasing concentration. Sample treated with 2.5 M NaOH which is the highest concentration provides highest dispersion of silica particles with mean particle size of 0.17  $\mu\text{m}$  as shown in Fig. 4 (c). This means that more concentrated NaOH solution is the best surface active substance to coat the surface uniformly. As a result, the extracted silica are well dispersed with uniform size and spherical shape of particles.

Whereas, SEM images for samples with varied heating time of 16 hours, 32 hours and 48 hours at fixed NaOH concentration and temperature are illustrated in Fig. 5. The particles are also in aggregated form. As the heating time is increasing, the particle size can be seen decreasing with 0.36  $\mu\text{m}$ , 0.19  $\mu\text{m}$  and 0.17  $\mu\text{m}$  respectively. It indicates that the longer time for heating will cause higher moisture content reduction and shrinkage of the silica particles at the same time. Thus, in this project, longest heating time is suggested, which is 48 hours, to produce the smallest particle size.

Fig. 6 provide SEM images at 250X and 10,000X magnifications between varied heating temperature ranging from 50°C, 80°C and 100°C with fixed NaOH concentration and heating time. It is observed that sample treated with the highest temperature that is 100°C exhibit the biggest mean particle size, exceeding 1.23  $\mu\text{m}$ , as compared to the other two, with 0.46  $\mu\text{m}$  and 0.17  $\mu\text{m}$  respectively. Thus, it clearly proves that higher heating temperature will lead to bigger size due to mild fusion and nucleation of particle happened at the surface as the temperature is increased from 50°C to 100°C. Hence, the optimum temperature for heating is the lowest, which is 50°C.



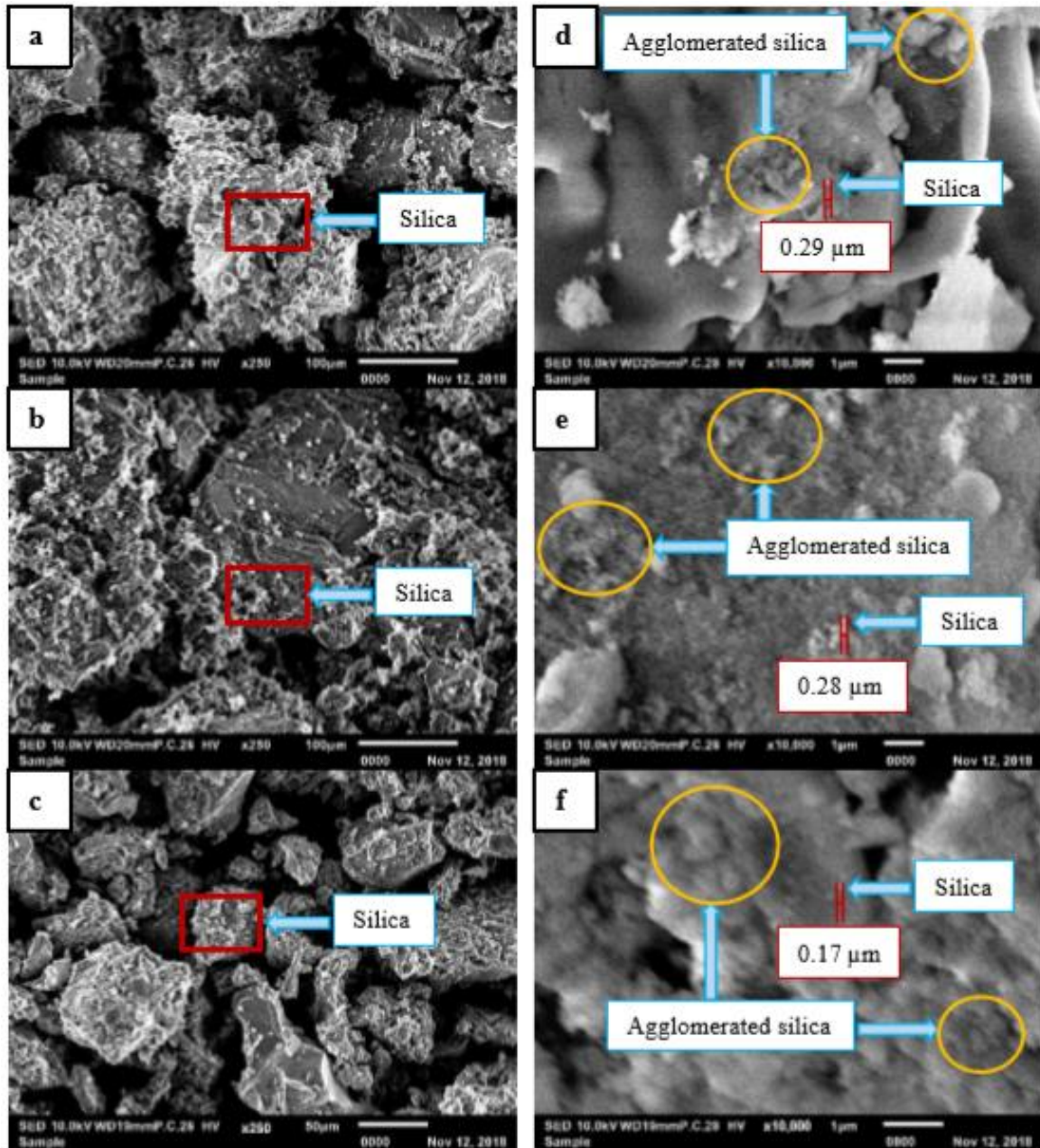


Fig. 4: SEM images at magnification of 250X for samples added with ; (a) 0.5 M NaOH (b) 1.5 M NaOH (c) 2.5 M NaOH and at magnification of 10,000X for samples added with ; (d) 0.5 M NaOH (e) 1.5 M NaOH (f) 2.5 M NaOH



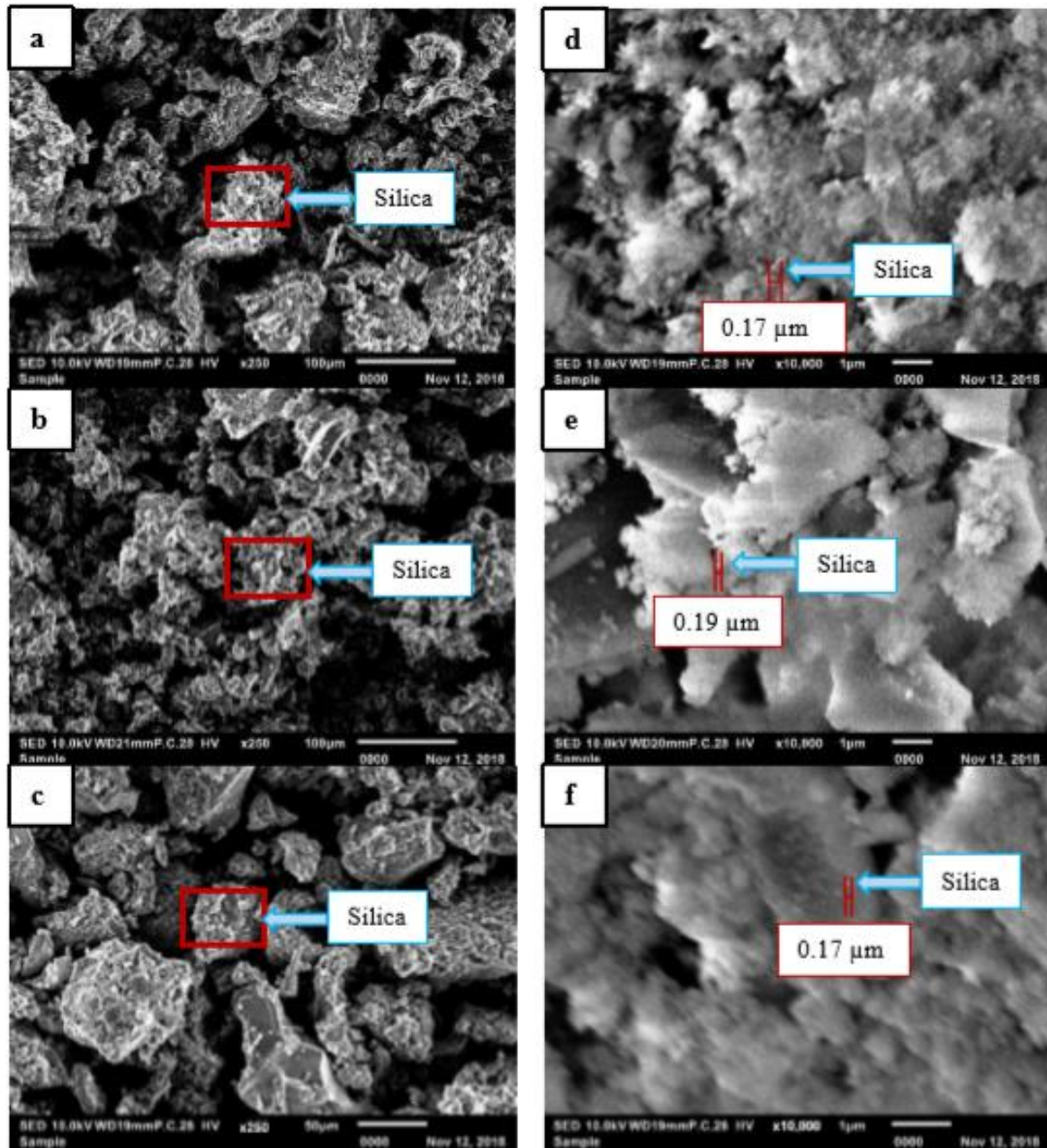


Fig. 5: SEM images at magnification of 250X for samples heated for ; (a) 16 hours (b) 32 hours (c) 48 hours and at magnification of 10,000X for samples heated for ; (d) 16 hours (e) 32 hours (f) 48 hours

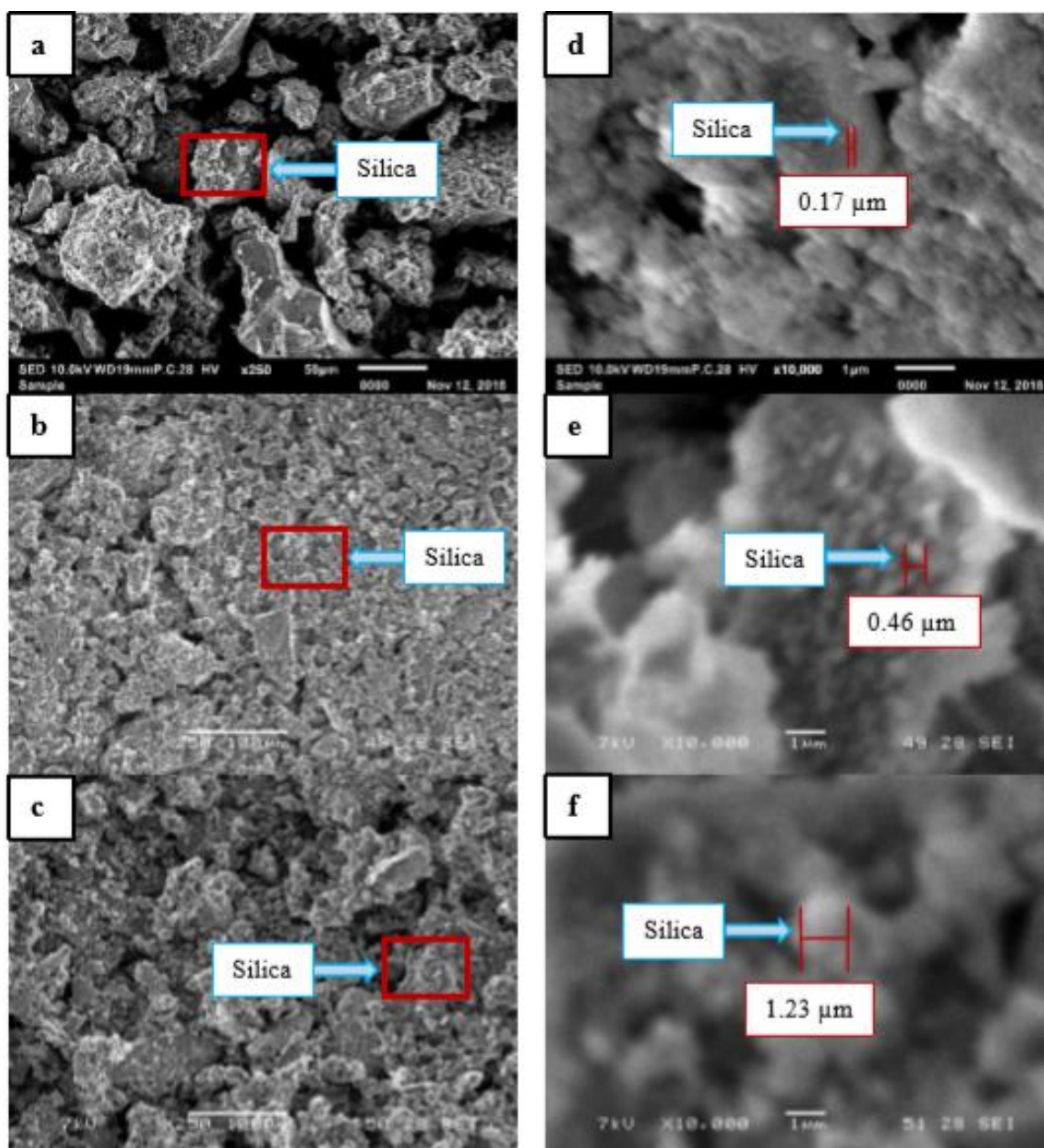


Fig. 6: SEM images at magnification of 250X for samples heated at ; (a) 50°C (b) 80°C (c) 100°C and at magnification of 10,000X for samples heated at ; (d) 50°C (e) 80°C (f) 100°C

To evaluate the condition of nanosilica particle even clearly and precisely, FESEM analysis has been done on one sample which have been selected based on the XRF, XRD and SEM results. It was found that the most optimum parameters to synthesis nanosilica powder from RHA are 2.5M NaOH, 48 hours and 50°C of heating. Thus, the FESEM images are illustrated in Fig.7 at magnification of (a) 10,000X and (b) 30,000X.

It can be seen that the silica particles are in circular shapes with mean diameter of 44.7 nm–85.6 nm, which can be classified as nano-sized particle because it is within the range of 1 nm–100 nm. Moreover, it has smaller range of particle size compared to sample treated with 100°C in Fig. 6 (c) which has mean particle size of 1.23 μm. This results indicate the effect of heating temperature which is increasing, leading to bigger size due to the nucleation that happened. During heating, energy has been absorbed by the particles which make them fused

with each other. Thus, as the temperature is increased, particle growth is also increased. Therefore, the lowest temperature is needed to heat the powder in order to produce smallest particle size [8]. Moreover, it is important to obtain smallest size of silica particle because it will exhibit higher surface area to volume ratio which results to higher reactivity in any particular applications that this nanosilica powder will be used in the future.

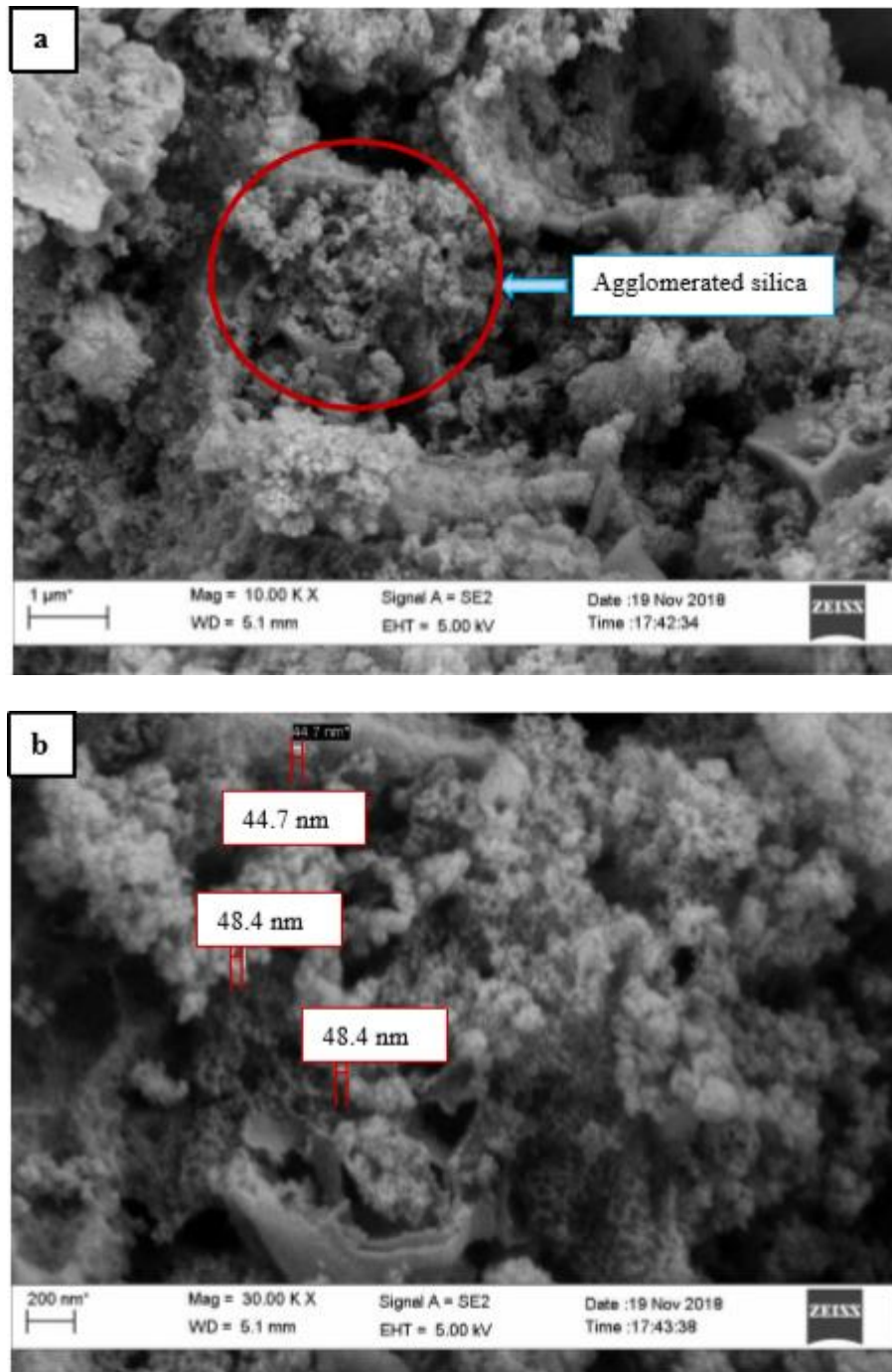


Fig. 7: FESEM images for sample treated with 2.5 M of NaOH, heated for 48 hours at 50°C, at magnification of: (a)10,000X and (b) 30,000X.

### Method 3



Raw materials which are calcium carbonate ( $\text{CaCO}_3$ ) and rice husk ash (RHA) are characterized using XRD analysis. The diffraction data were recorded in the  $2\theta$  range of  $20^\circ$ – $50^\circ$  with scanning rate of 0.25s/step. Characterization of raw materials which are calcium carbonate and rice husk ash have been done using XRD. Fig. 1 shows XRD patterns of commercial calcium carbonate ( $\text{CaCO}_3$ ) in accordance to standard diffraction of  $\text{CaCO}_3$ . Peak (104) revealed the highest amount of  $\text{CaCO}_3$  [6]. All values of crystal lattice at the diffraction peaks are in accordance with the standard XRD patterns of calcium carbonate. XRD pattern of rice husk ash (RHA) is present in Fig. 2 and shows a broad peak located approximately at  $2\theta = 21.5^\circ$ , that suggest an amorphous characteristic of the raw material and agrees with the reported data.

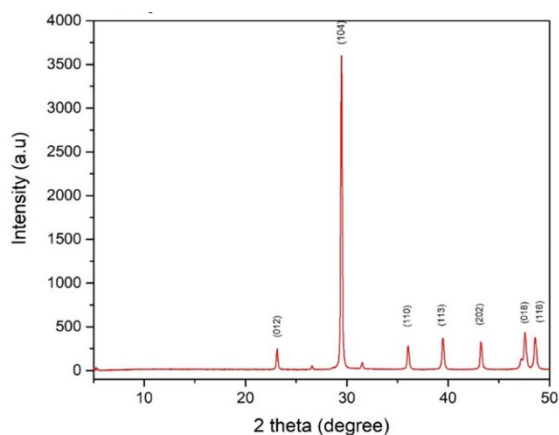
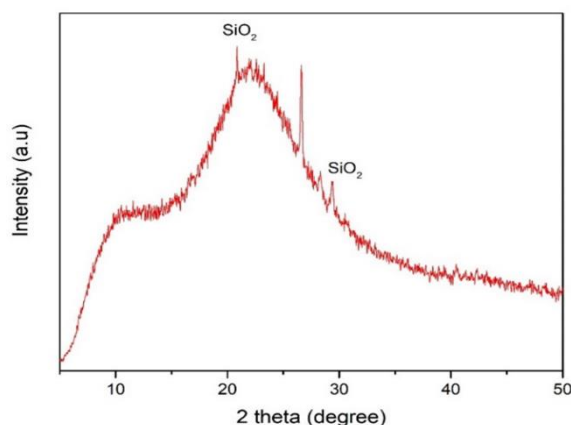
Fig. 1: XRD patterns of  $\text{CaCO}_3$ 

Fig. 2: XRD patterns of RHA

Fig. 3 (a) is the XRD patterns of prepared  $\text{CaO-SiO}_2$  sorbent with different weight composition. There are several elements contained in the sorbent such as  $\text{CaO}$ ,  $\text{SiO}_2$ ,  $\text{Ca}_2\text{SiO}_4$  (larnite) and  $\text{CaSiO}_3$  (calcium silicate). Larnite, formed by the reaction of  $\text{CaCO}_3$  and  $\text{SiO}_2$ , generally exhibits good chemical durability and high Tamman temperature of  $929^\circ\text{C}$  and can act as an ideal inert support to prevent  $\text{CaO}$ -based sorbent sintering [2]. Therefore, cyclic  $\text{CO}_2$  uptake over multiple carbonation-calcination processes of the synthetic sorbents could be enhanced.

The continuation of XRD analysis has been done for  $\text{CaO-SiO}_2$  sorbents at different grinding times after calcined at  $700^\circ\text{C}$ . Elements such as  $\text{SiO}_2$ ,  $\text{CaO}$  and calcite ( $\text{CaCO}_3$ ) exist in the sorbents as shown in XRD pattern (Fig. 3 (b)). Each sorbent seems to have almost same XRD peak but with different intensity. Based the XRD patterns of the sorbents, there are intense peak observed at  $2\theta$  equals to  $29.55^\circ$ ,  $36.04^\circ$  and  $43.25^\circ$ .  $\text{CaO-SiO}_2$  sorbent that has been calcined at  $700^\circ\text{C}$  has highest intensity of XRD peak at (104) with element of calcite. Calcite is the mineral contained in calcium carbonate ( $\text{CaCO}_3$ ). Meanwhile,  $\text{SiO}_2$  element is observed at  $2\theta$  equals to  $43.25^\circ$ . Based on the XRD patterns obtained from this analysis, it

can be said that the prepared CaO-SiO<sub>2</sub> sorbents have been fully transform into crystalline structure.

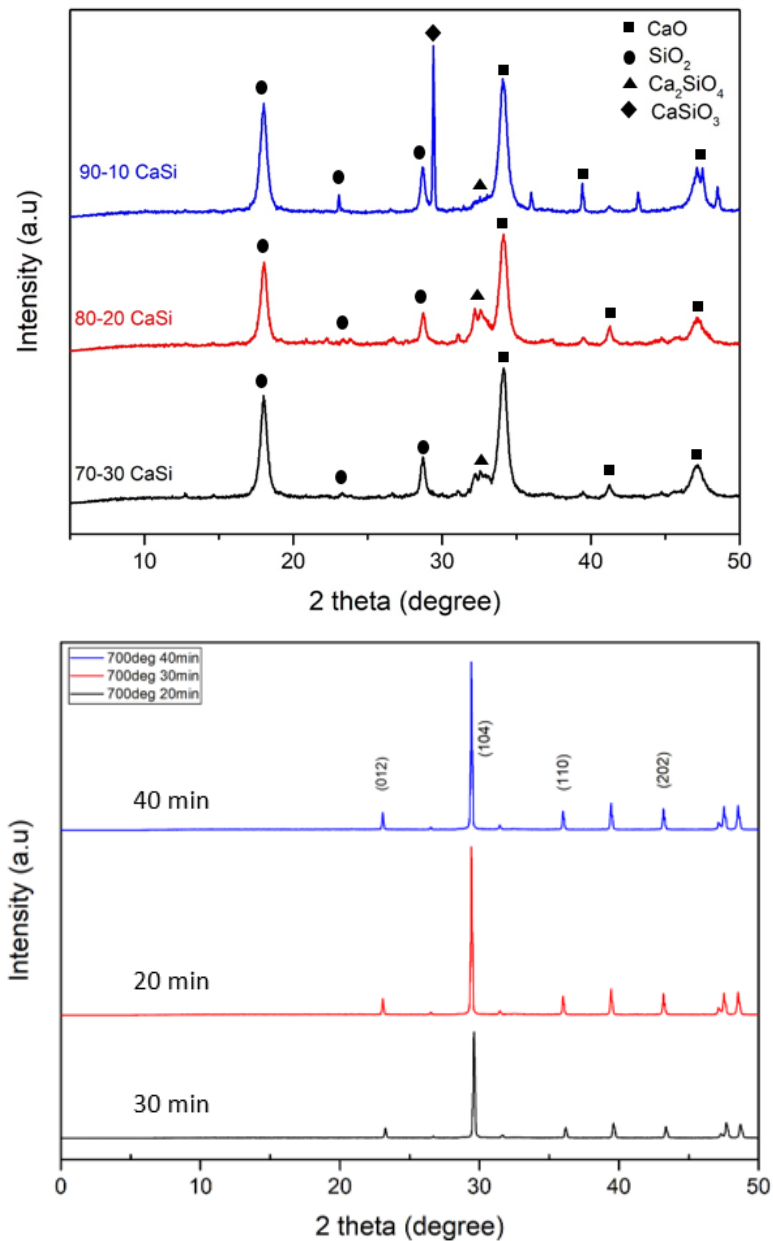


Fig. 3: XRD patterns of CaO-SiO<sub>2</sub> before calcined at (a) different weight ratio and (b) after calcined at 700 °C (90:10) with different grinding times

Three samples of CaO-SiO<sub>2</sub> with different weight percent of CaCO<sub>3</sub>-RHA (90:10, 80:20 and 70:30) are characterized using SEM as in Fig.4. Based on the SEM images, CaO-SiO<sub>2</sub> with composition CaCO<sub>3</sub> - RHA (90:10) has bigger particle size with irregular shape with some porosity. Besides that, the particle itself does not agglomerate with each other.

Meanwhile, Fig. 4(b) shows the surface morphology of CaO-SiO<sub>2</sub> with composition CaCO<sub>3</sub>-RHA (80:20). The SEM image shows that the sorbent has smaller particle size with plate-like structure and has less porosity. The particles seem to be well dispersed compared to CaO-SiO<sub>2</sub> sorbent (90:10). Then, Fig. 4(c) illustrates SEM images for CaO-SiO<sub>2</sub> with composition CaCO<sub>3</sub>-RHA (70:30). The result shows that agglomeration between particles occur in preparation of CaO-SiO<sub>2</sub> sorbent.

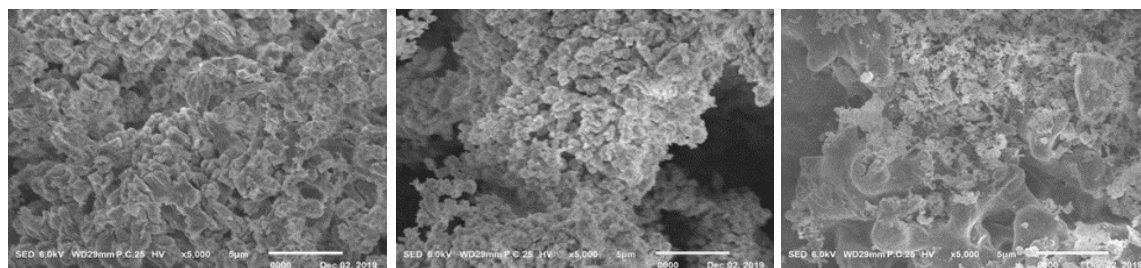


Fig. 4: Morphology CaO-SiO<sub>2</sub> sorbents with different weight ratio; (a) 90:10, (b) 80:20, (c) 70:30

Fig. 5 illustrates the SEM images of respective CaO-SiO<sub>2</sub> sorbents for 90:10 weight ratio after calcination at 700 °C. SEM images show remarkable changes in morphology and its porous nature [7]. For CaO-SiO<sub>2</sub> sorbents calcined at 700 °C with 20 mins grinding time exhibits small size of particles with some porosity. Besides that, the particles are well distributed without agglomeration occur. The conventional morphology of CaCO<sub>3</sub> polymorph, known as aragonite is “needle-like” structure. However, the shape may change into “flake-like” or “cauliflower-like” structure as shown in Fig. 5(a) restricted to certain crystallization condition [8]. SiO<sub>2</sub> particles are “tiny” spherical ones and can be observed in Fig.5(b) [9]. Slight agglomeration also appeared at several spots in the sorbent structure when the sorbent was grinded for longer time, hence result in larger size of particles produced as shown in Fig. 5(c). Agglomeration of the sorbent particles could lead to the pore blockage and narrowing the sorbent reactivity along the multiple carbonation-calcination cycles [10]. Porous nature of the sorbents help in increasing the CO<sub>2</sub> sorption capacity of the adsorbents.

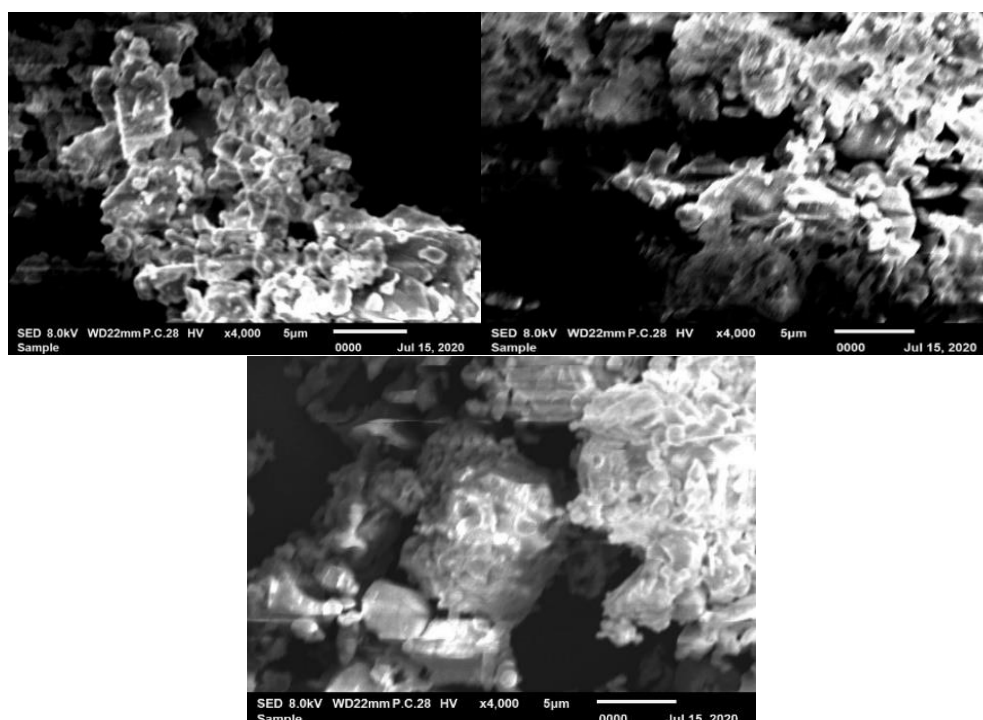


Fig. 5: Morphology of CaO-SiO<sub>2</sub> sorbent calcined at 700 °C with different grinding time; (a) 20 min, (b) 30 min and (c) 40 min

Fig. 6 shows the cyclic CO<sub>2</sub> sorption capacity of the sorbents calcined at 700 °C with different grinding times. The calcined CaO-SiO<sub>2</sub> sorbents were tested for 20 consecutive carbonation and calcination cycles. The overall adsorption performance of the sorbents depends on the cyclic capacity of CO<sub>2</sub> capture [12]. As shown in Figure 4.17, the cyclic CO<sub>2</sub> sorption capacity decreased dramatically as the time of grinding increased from 20 minutes to 30 minutes. Sorbent calcined at 700°C and grinded for 20 minutes exhibits more stable structure for CO<sub>2</sub> capture system. Based on the TG curve of the sorbents, there is approximately 20 percent of CO<sub>2</sub> adsorption occur during the Thermogravimetric Analysis (TGA). Sorbent with more stable structure is able to capture more CO<sub>2</sub> and withstand the multiple adsorption-desorption cycles. High calcination temperature accelerates the sintering of sorbents during cyclic carbonation and calcination reactions [11]. This reduction occurs due to the sintering effect of the sorbents. Sintering caused grain growth which means increasing the average grain size and also minimize the pore openings [13]. Sintering phenomenon occurs because of high temperature involved during carbonation and calcination cycles which degrade the CO<sub>2</sub> uptake performance of the samples [2]. Thus, CaO-SiO<sub>2</sub> sorbent treated with 700 °C calcination temperature and 20 minutes of grinding shows better cyclic CO<sub>2</sub> sorption capacity compared to other samples.

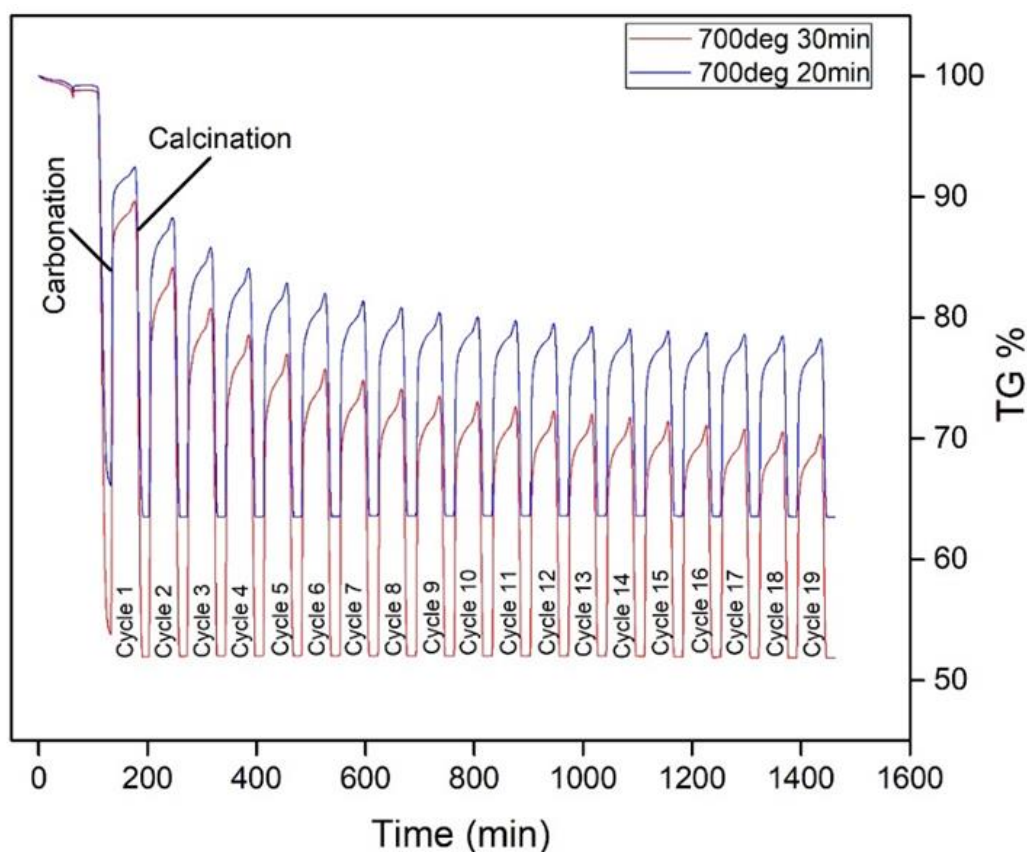


Fig. 6: TGA curve of CaO-SiO<sub>2</sub> calcined at 700 °C with different grinding times

Then, the TG analysis has been done for the CaO-SiO<sub>2</sub> sorbents with different calcination temperature but same time of grinding. As shown in Figure 4.18, the CO<sub>2</sub> adsorption of the sorbents drop drastically until 600 minutes and after that the sorption capacity of the sorbents remain almost the same until reach 20 cycles of calcination and carbonation. Meaning that, the addition of silica into the calcium-based sorbents enhance the cyclic stability and CO<sub>2</sub> uptake of the calcium-based sorbents. However, due to high calcination temperature, sorbent treated with 800 °C of calcination shows rapid decay in cyclic CO<sub>2</sub> capture capacity compared to sorbent treated with 700 °C of calcination. This reduction occurred due to the sintering effect of the sorbents. Sintering caused grain growth which means increasing the average grain size and minimize the pore openings (Mahinpey et al., 2016). As mentioned before in Chapter 1, sintering phenomenon occurs because of high temperature



involved during carbonation and calcination cycles which degrade the CO<sub>2</sub> uptake performance of the samples. Thus, CaO-SiO<sub>2</sub> sorbent treated with 700 °C calcination temperature and 20 minutes of grinding shows better cyclic CO<sub>2</sub> sorption capacity compared to other samples. Low calcination temperature meaning that low energy is used, however can produced CaO-SiO<sub>2</sub> sorbents with stable and high cyclic CO<sub>2</sub> adsorption.

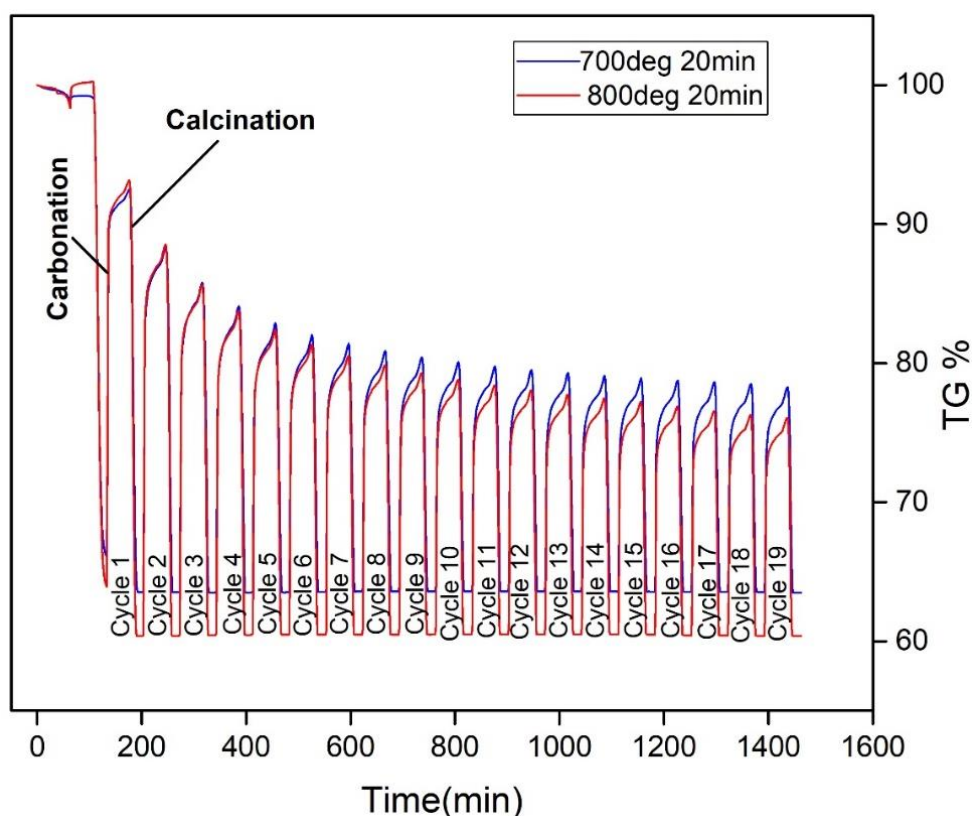


Fig. 7: TG curve of CaO-SiO<sub>2</sub> sorbents with vary calcination temperature

#### Method 4

##### *Analysis on the Raw Materials*

Fig. 1(a) and 1(b) show the XRD pattern of Ca(OH)<sub>2</sub> and RHA at different scale of intensity. Based on the Fig. 1(a), sharp peaks at  $2\theta = 18.1^\circ$ ,  $29.45^\circ$ ,  $34.15^\circ$ ,  $47.25^\circ$  and  $50.85^\circ$  proved the crystalline structure of Ca(OH)<sub>2</sub>. Whereas Fig. 1(b) indicated broad peak, centered at about  $2\theta = 23^\circ$  which confirms the amorphous structure of RHA. It is common that silica contain in RHA has amorphous structure, and its transformation to crytalline structure will occur when temperature is increased beyond 700°C [9].

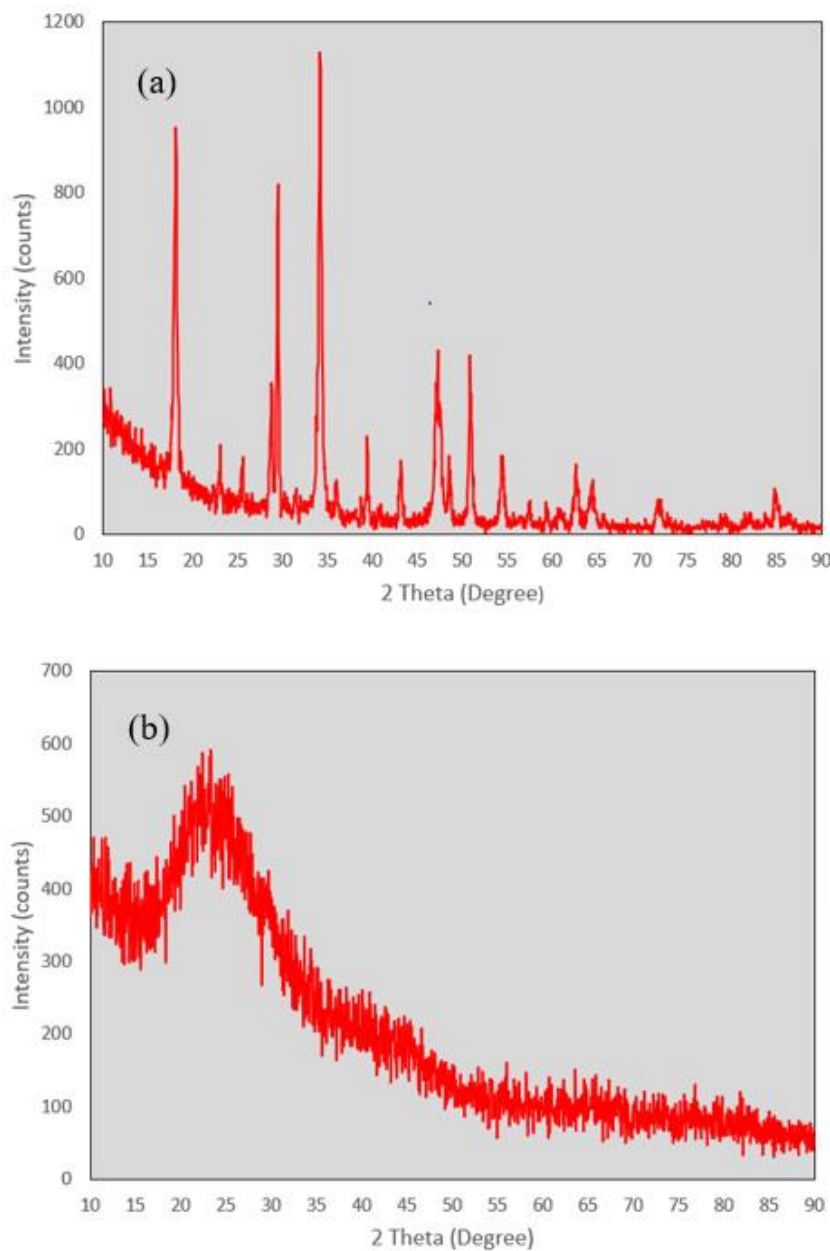


Fig.3. XRD pattern of a)  $\text{Ca(OH)}_2$  and b) RHA

Fig. 2 and 3 displayed the SEM micrographs of  $\text{Ca(OH)}_2$  and RHA. It has been observed for  $\text{Ca(OH)}_2$  that it consists of finely dispersed, small size particles. Under X5000 magnification (Fig. 2(c)), the morphology of  $\text{Ca(OH)}_2$  revealed that the microstructure is in granular and agglomerated shape. While for RHA, the SEM images reveal the siliceous nature and with some porosity of the ashes. It was observed that RHA has agglomerated particles in various sizes and irregular structures.

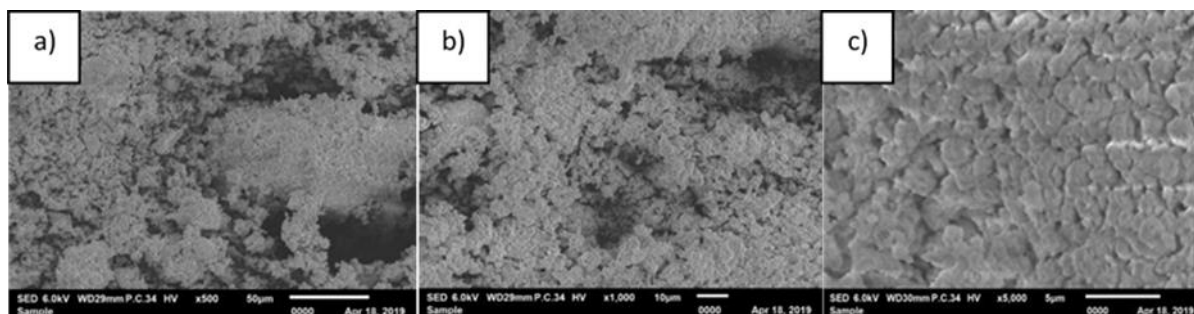


Fig. 4. SEM micrographs of  $\text{Ca}(\text{OH})_2$  at magnification of a) 500X, b) 1000X and c) 5000X

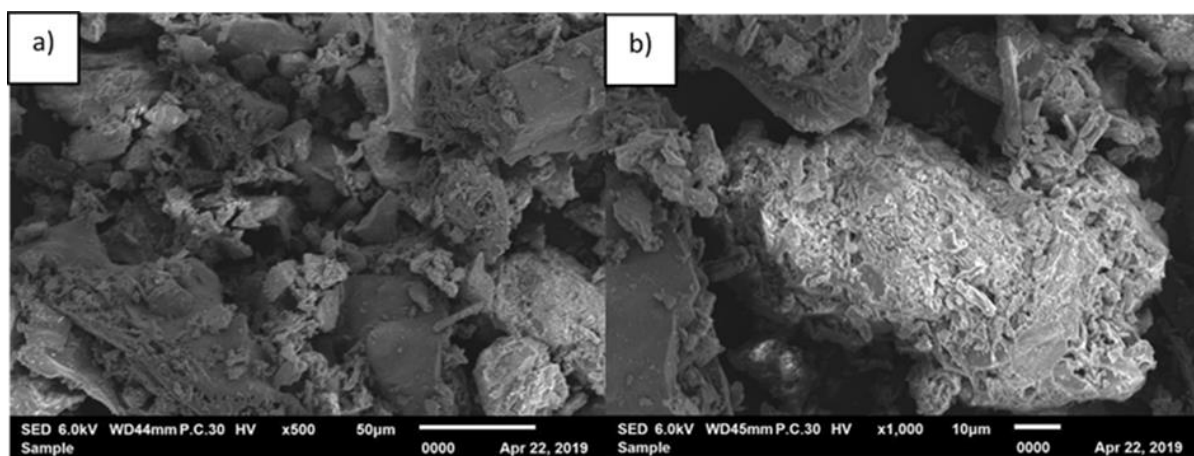


Fig 5: SEM micrographs of RHA at magnification of a) 500X and b) x1000X

### ***Characterization of the Sorbent Pellets***

#### ***Average Size of the Pellets***

Fig. 4 (a) and (b) show the different ratio of  $\text{CaO-SiO}_2$  pellets obtained from the granulation process. As shown in Fig. 4 (a) and (b), the average size of particles for 80:20 and 70:30 pellets are 3.0 mm and 4.5 mm respectively. The utilization of high speed of granulator and optimum amount of deionized water added during the granulation process resulted in small size of pellets. A small size of pellets was desired as the smaller the pellets, the higher the surface area of the pellets to covered for potential  $\text{CO}_2$  adsorption application. However, the significant difference in the average particles size among the two ratios is presumed to occur due to the different amount of RHA, as the  $\text{SiO}_2$  source added in  $\text{CaO-SiO}_2$  pellets. The smaller size of pellets is obtained when lower amount of RHA added. Table 2 summarized the details of granulation process and the resulted average particles size for each ratio before undergo calcination process at  $750^\circ\text{C}$ .

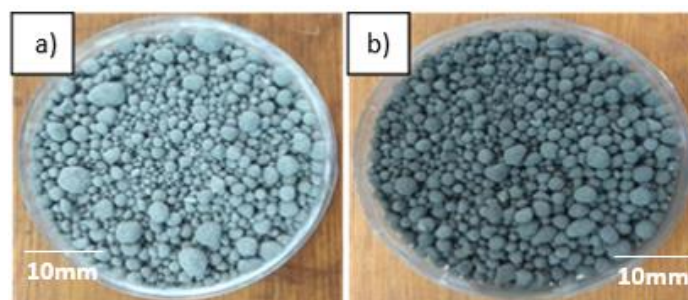


Fig. 4 .The obtained pellets from the granulation process of (a) ratio 80:20 and (b) ratio 70:30.

Table 2: Summary of the pellets obtained from two different ratios.

Ratio of $\text{Ca(OH)}_2$ and RHA	Impeller and Chopper Speed (rpm)	Amount of Deionized Water (ml)	Average Size (mm)
80:20	73, 1700-1800	300	3.0
70:30	73, 1700-1800	300	4.5

Fig. 5 shows that  $\text{CaO-SiO}_2$  pellets after the calcination process at  $750^\circ\text{C}$ . As can be observed in Fig. 5, all pellets have significant reduction in the size of pellet which is much smaller compared to the one before the calcination. This is probably due to the elimination of moisture from the pellets and significant reduction/shrinkage in pellets size after the calcination indicates huge amount of moisture content in each pellets.

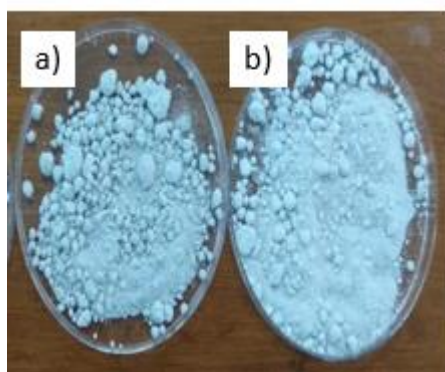


Fig. 5. Pellets after calcination of different ratio ;(a) 80:20 and (b) 70:30.

### ***Different Ratio of $\text{CaO-SiO}_2$ Pellets Before Calcination***

The phase structure of  $\text{CaO-SiO}_2$  pellets for each ratio before the calcination process was characterized by XRD analysis, as displayed in Fig. 6 (a) and (b). The peak characteristics of  $\text{Ca(OH)}_2$  and  $\text{SiO}_2$  are detected in XRD pattern of all  $\text{CaO-SiO}_2$  pellets. According to Fig. 6, it is evident that the main crystalline peaks of  $\text{Ca(OH)}_2$  were detected at about  $2\theta = 28.76^\circ$ ,  $34.17^\circ$ ,  $47.21^\circ$  and  $62.78^\circ$ . However, the intensity for each peak was decreased with increasing

amount of RHA added. Besides, the characteristics peak of silica also could be observed from the XRD pattern, however, the intensity of the peaks was very low due to its amorphous nature. The silica peak centered about  $2\theta = 23^\circ$  was observed in both XRD spectras of pellets prepared.

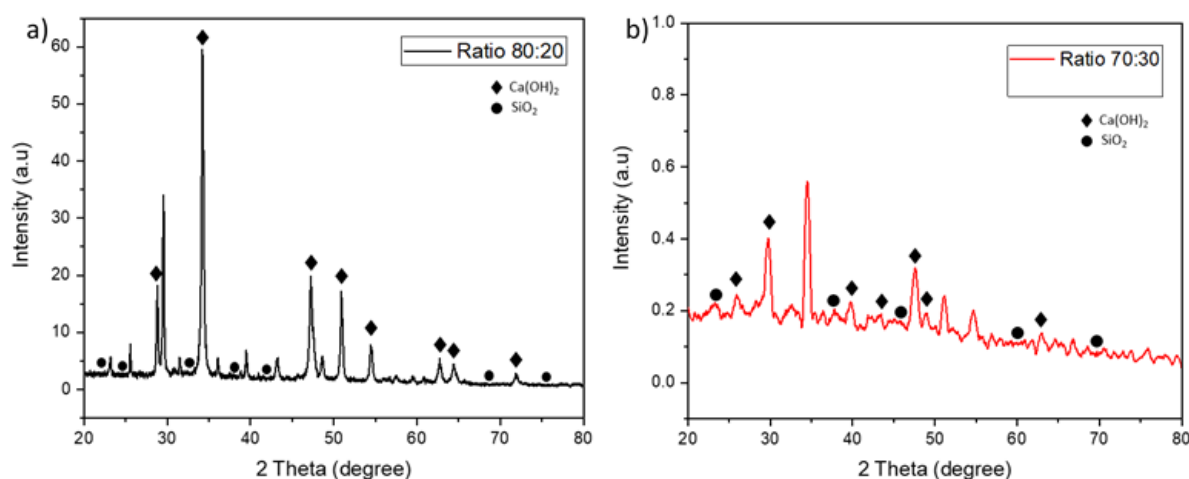


Fig. 6. XRD spectra for different ratio of CaO-SiO<sub>2</sub> before calcination, (a) 80: 20 and (b) 70:30

Different ratio of RHA addition in the CaO-SiO<sub>2</sub> pellets as the biomass sacrificial template did not disrupted the crystalline structure of the calcium precursor. This is proved by the almost similar XRD pattern obtained from the CaO-SiO<sub>2</sub> pellets with the XRD pattern of the raw Ca(OH)<sub>2</sub>. Besides, the detection of similar major diffraction peaks from XRD pattern of all pellets evidenced the incorporation of sacrificial biomass template materials did not modify the crystallinity of the pellets produced [8].

The SEM micrograph of the prepared CaO-SiO<sub>2</sub> pellets at different ratios were shown in Fig. 7 and 8. All the micrographs illustrated that addition of RHA had significantly altered the morphology of CaO-SiO<sub>2</sub> pellets prepared, according to the ratio. Based on Fig. 8, 80:20 pellet shows large and irregular grains size with random distribution. Meanwhile, 70:30 pellet exhibits randomly distributed, irregular, and smaller shape of microstructures. Some small needle-like or flake structure could be observed which indicates the presence of ash or biomass material inside the pellets that have been prepared. According to the micrographs obtained, increasing amount of RHA added caused the grains size to decrease significantly which lead to the development of irregular microstructures.



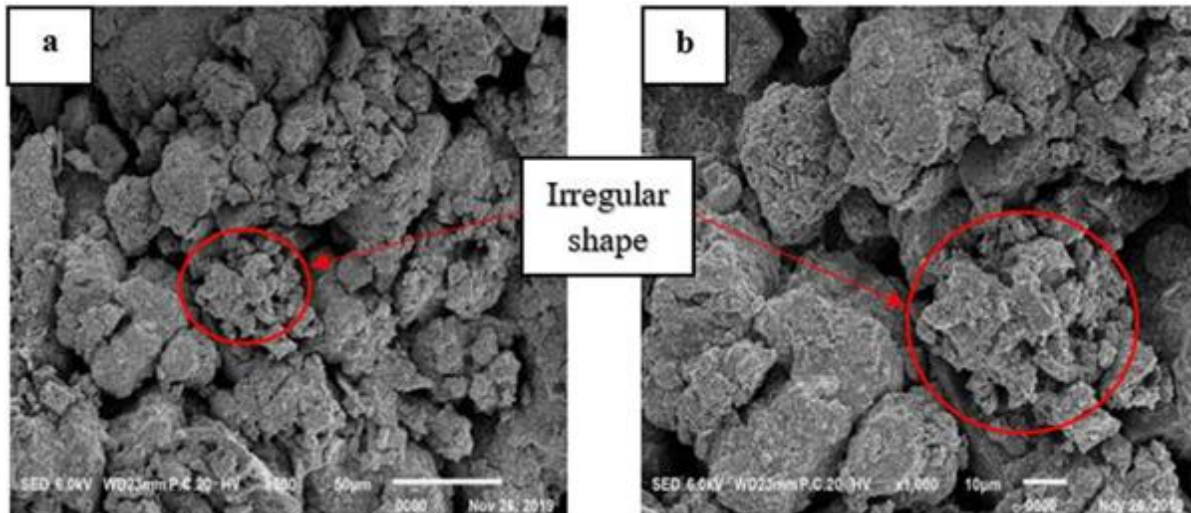


Fig.7. SEM micrographs of CaO-SiO<sub>2</sub> pellets ratio 70:30 before calcination at different magnification a) 500X and b) 1000X

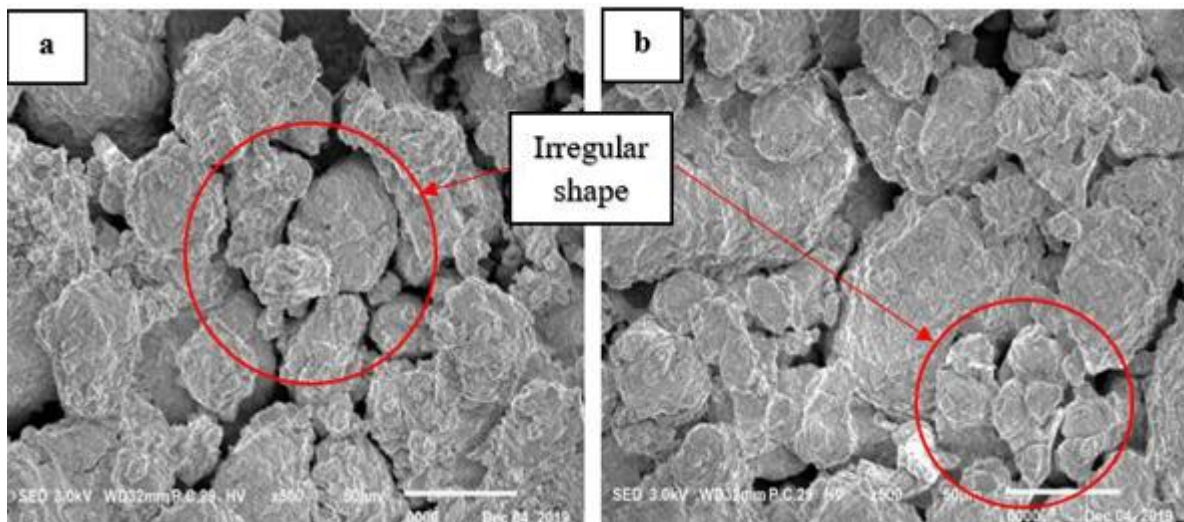


Fig.8. SEM micrographs of CaO-SiO<sub>2</sub> pellets ratio 80:20 before calcination at two different spots by magnification of 500X

### ***Effect of Different Ratio after 750 °C Calcination***

The effect of calcination at 750°C on the phase structure of CaO-SiO<sub>2</sub> pellets prepared is shown in Fig. 9. Sharp peaks were detected from all of the XRD pattern obtained which confirmed the existence of crystalline phase. This is due to the formation of CaO after sintering at 750°C. The CaO peaks can be observed at  $2\theta = 29.76^\circ, 33.02^\circ, 39.49^\circ, 47.56^\circ, 51.91^\circ$  and  $54.58^\circ$ . However, there is significant difference in intensity of peak at  $2\theta = 29.76^\circ$ . The highest peak intensity was observed in 70:30 pellet followed by 80:20 pellet. Supposedly, if the amount of CaO is higher compared to the silicate, the significant increment in peak intensity of CaO should be obtained whereas the silicate peaks should remain unchanged [10].

But from the XRD pattern obtained, pellet with low amount of CaO (70:30 pellet specifically) possessed the highest peak of CaO. This is presumed to occur due to the calcination process at 750°C might have altered the phase structure of silica in RHA and thus modified the XRD pattern of all pellets.

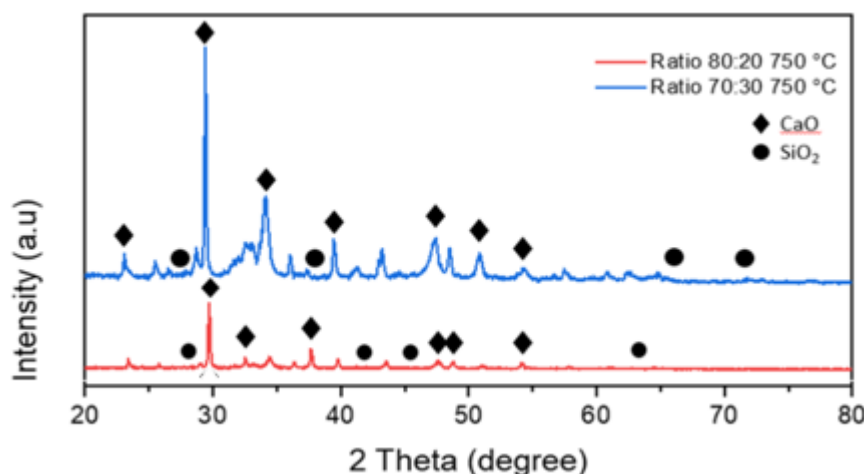


Fig.9. XRD spectra for different ratio of CaO-SiO<sub>2</sub> pellet calcined at 750°C

Morphology of the calcined CaO-SiO<sub>2</sub> pellets for each ratio are shown in Fig. 10 and 11. After calcination at 750°C, the formation of pores was observed in micrographs acquired. For 80:20 pellet, grains with random sized have been developed after sintering at 750°C with the presence of needle-like structure. The presence of needle-like structure suggests formation of a new compound resulted from the calcination of CaO-RHA which mainly composed of Ca, Si and O elements [11]. As for 70:30 pellet, the morphology consists of randomly scattered grains which is small in size as shown in Fig. 11. 70:30 pellet has irregular pores structure but not as large as compared to the pore structure in 80:20 pellet. However, 80:20 pellet shows better porosity as the pores size were larger which caused an increased in porosity. Higher amount of well-structured pores were more preferred for CO<sub>2</sub> capture application; in which it would contribute to an excellent performance of CO<sub>2</sub> adsorption.

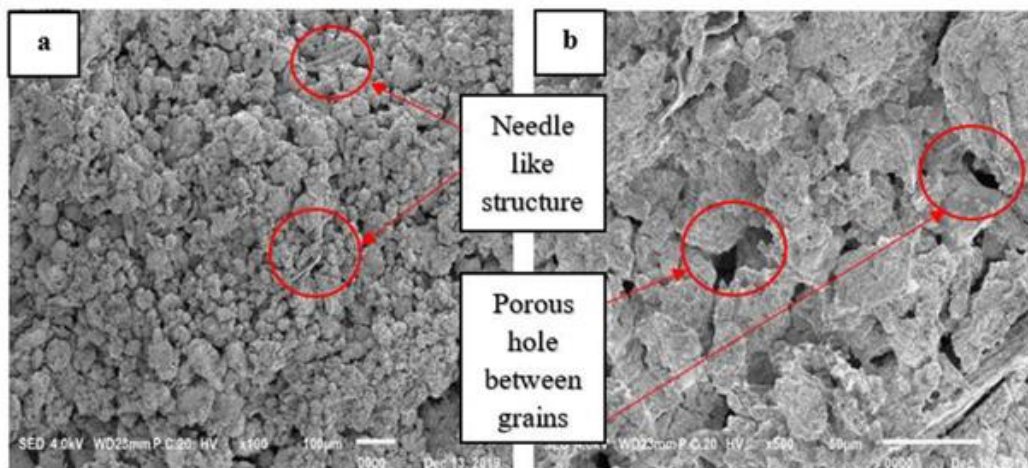


Fig.10. SEM micrographs of CaO-SiO<sub>2</sub> pellets ratio 80:20 after calcination at 750°C with different magnification a) 100X and b) 500X.

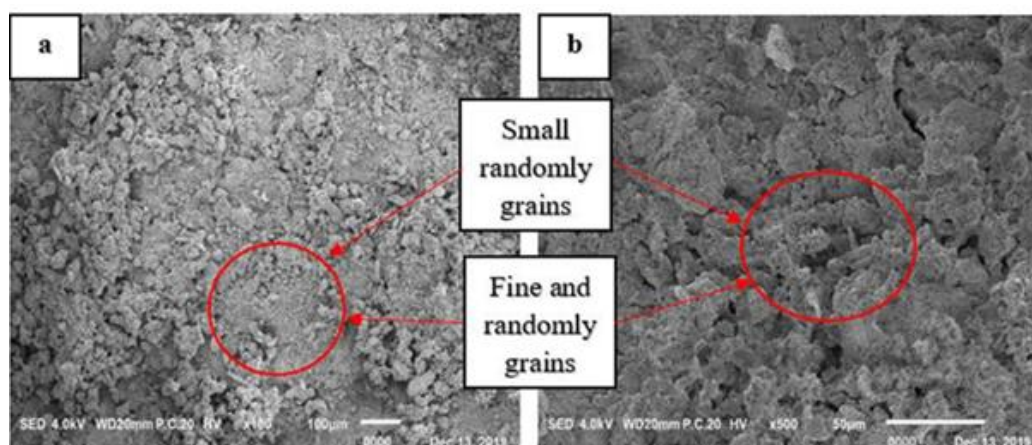


Fig.11. SEM micrographs of CaO-SiO<sub>2</sub> pellets ratio 70:30 after calcination at 750 °C with different magnification a) 100X and b) 500X.

### Conclusion:

In a conclusion, Ca-based MgO hybrid adsorbent had been successfully synthesized by two-step method. This method is much easier compared to other methods which are complex. These samples have been characterized with Scanning Electron Microscope (SEM) and X-Ray Diffraction (XRD). For SEM analysis, it is observed that both samples have irregular spherical to granular shape. Moreover, it is found that the sorbent has more porosity which will contribute to the efficiency of adsorption capacity of CO<sub>2</sub> capture. XRD analysis showed the existence of CaO and MgO in the sorbent and Ca-based MgO that had been calcined at 650°C has higher intensity peak compared to 550°C. FTIR analysis showed presence of Ca—O



bond and Mg=O bond. This showed that Ca-based MgO hybrid adsorbent calcined at 650°C has a good crystallinity.

High purity of fine nanosilica powder (100% purity) with amorphous structure was successfully extracted from RHA started from pre-synthesis process involved acid leaching with HCl, followed by thermal treatment. Then, the RHA was subjected to precipitation method by the addition of NaOH and H<sub>2</sub>SO<sub>4</sub> to neutralize the solution, which finally yielded a dried precipitate of silica. Meanwhile the broad peaks have been demonstrated indicating that all of the synthesized silica powder samples are in amorphous state. The silica particle yielded in this work are in uniform spherical shape and the distribution is found to be uniform. It tends to agglomerate with mean particle size ranging from 44.7 nm to 1.23 µm. The smallest size was achieved from the sample treated with 2.5 M NaOH, and heated at 50°C for 48 hours, which is the similar sample that yield the best results from XRF. Therefore, the optimum parameters to be used are 2.5 M of NaOH and then heated at 50°C for 48 hours, which confirmed the quality of high purity and smallest size of nanosilica powder extracted from RHA.

Furthermore, synthetic CaO-SiO<sub>2</sub> adsorbent had been successfully prepared by using physical dry mixing method which is much simpler compared to other available methods like sol-gel and co-precipitation. These sorbents were characterized using Scanning Electron Microscopy (SEM), X-Ray Diffraction (XRD) and Fourier Transform Infrared (FTIR) spectroscopy as a preliminary result for this research. From SEM analysis, it can be observed that all the samples have different porosity, size and shape of particles and particles distribution. Moreover, it is found that the sorbent with more porosity will contribute to high efficiency of adsorption capacity of CO<sub>2</sub> capture. Besides that, XRD patterns of the prepared sorbents show new crystalline phase, larnite (Ca<sub>2</sub>SiO<sub>4</sub>), which possess good chemical durability and may help to prevent sintering effect of calcium based sorbent. Thermogravimetric Analysis (TGA) evaluate that sorbent treated with 700 °C of calcination and 20 minutes of grinding exhibits stable sorbent reactivity for cyclic CO<sub>2</sub> capture.

The CaO-based pellets with addition of RHA as the sacrificial bio-template had been successfully prepared via granulation method. The calcium precursor, Ca(OH)<sub>2</sub> has agglomerates and granular microstructures and RHA has an irregular and in definitive shape of microstructures. Based on the XRD analysis, the Ca(OH)<sub>2</sub> has crystalline structure, while RHA has amorphous structure. XRD analysis proved that the inclusion of RHA in the Ca(OH)<sub>2</sub> did not disrupted the crystalline structure of the samples and intensity of the peaks

were reduced with increasing amount of RHA added. However, the calcination at 750°C has significantly modified the XRD pattern of all CaO-SiO<sub>2</sub> pellets. The sharp peaks indicated the development of crystalline CaO and different ratio has different peak intensity. The pellets with low amount of RHA has finer grain structure observed as for increased the amount of RHA caused the pores became agglomerate, increase in size and randomly distributed. To conclude, based from the characterization result it indicates that ratio 80:20 and calcination temperature of 750 °C were the optimum parameters to be used for the pellets production.

## **Output:**

### **8 publications**

Farah Diana Mohd Daud, Nur Aishah M. Azmy, Mudrikah Sofia Mahmud, Norshahida Sarifuddin, Hafizah Hanim Mohd Zaki, Preparation of Nanosilica Powder Using Rice Husk via Precipitation Method, Materials Science Forum ,2020, Vol. 1010, pp 501-507(Scopus)

Farah Diana Mohd Daud, Nurul Amirah Izzati Ahmad, Mudrikah Sofia Mahmud, Norshahida Sariffudin, Hafizah Hanim Mohd Zaki, Two-Step Synthesis of Ca-Based MgO Hybrid Adsorbent for Potential CO<sub>2</sub> Capturing Application, Materials Science Forum ,2020, Vol. 981, 369-374 (Scopus)

Farah Diana Mohd Daud, Nur Aishah M. Azmy, Mudrikah Sofia Mahmud, Norshahida Sarifuddin, Hafizah Hanim Mohd Zaki, Preparation of CaO-SiO<sub>2</sub> Adsorbent for Potential CO<sub>2</sub> Capture via Dry Mixing Method, Material Science Forum ,2020 (Accepted) (Scopus)

Farah Diana Mohd Daud, Nur Aishah M. Azmy, Mudrikah Sofia Mahmud, Norshahida Sarifuddin, Hafizah Hanim Mohd Zaki, Preparation Of Cao-Based Pellet Using Rice Husk Ash Via Granulation Method For Potential CO<sub>2</sub> Capture, IIUM Journal, IIUM Engineering Journal, Vol. 22, No.1, 2021 (Scopus)

Farah Diana Mohd Daud , Muhammad Hilmi Johari , Afiq Haikal Ahmad Jamal , Nor Amyra,Zulianey Kahlib , and Assayidatul Laila Hairin, Preparation of nano-silica

powder from silica sand via sol-precipitation method, IAP Conference Proceeding, 2068, 020002 (2019)

Hafizah Hanim Mohd Zaki, Nur Azemuzahir Mohd Sobri, Jamaluddin Abdullah, Norshahida Sarifuddin, Farah Diana Mohd Daud, Characterization of NiTi Shape Memory Alloy Sintered at Different Temperatures in Reducing Environment, Materials Science Forum, 2020, Vol. 1010, pp 632-637 (scopus)

Ikhwan Yusuff, Norshahida Sarifuddin\*, Afifah Mohd Ali, Farah Diana Mohd Daud and S. Norbahiyyah, A Comparative Study on Mechanical Properties of Carbon and Kenaf Composites via Vacuum Infusion Technique, Journal of Engineering Science, Vol. 16(1), 97–107, 2020.

Assayidatul Laila Nor Hairin, Mohd Fitri Idris, Raihan Othman, Farah Diana Mohd Daud, Alya Naili Rozhan, and Hafizah Hanim Mohd Zaki, Effect of Acceptor Impurity (Cu and Al) in Zn<sub>4</sub>Sb<sub>3</sub> Thermoelectric Materials via Hot-isostatic Pressing (HIP) Method, IAP Conference Proceeding, 2068, 020008 (2019)

### **Future Plan of the research:**

There are some improvement need to be done for my current research for better results and findings. This project can be further study in terms of silica sources. There are many other sources of silica such as nanosilica powder and fume silica that can be used to replace RHA. The CO<sub>2</sub> setup should be developed to investigate CO<sub>2</sub> adsorption instead of using TGA analysis only.

### **References:**

- 1) D. Shekhawat, D. R. Luebke and H. W. Pennline, “A Review of Carbon Dioxide Selective Membranes,” US Department of Energy, NETL-1200, 2003, pp. 9-11.
- 2) Y. S. Lin, A. J. Burggraaf, J. Amer. Ceram. Soc. 1991, 74, 29.
- 3) K. K. Chan, A. M. Brownstein, Amer. Ceram. Soc. Bull. 1991, 70, 703.
- 4) M. Karkare, “Nanotechnology: Fundamentals and Applications,” IK International Pvt Ltd., 2008, p. 12.
- 5) Anon., 2011. [http://CO<sub>2</sub>now.org/Current-CO<sub>2</sub>/CO<sub>2</sub>-Now/global-carbon-emissions.html](http://CO2now.org/Current-CO2/CO2-Now/global-carbon-emissions.html)

- 6) Othman, M.R., Tan, S.C., Bhatia, S., 2009. Separability of carbon dioxide from methane using MFI zeolite-silica film deposited on gamma-alumina support. *Microporous and Mesoporous Materials* 121, 138–144.
- 7) Yang, H., Xu, Z., Fan, M., Gupta, R., Slimane, R.B., Bland, A.E., Wright, I., 2008. Progress in carbon dioxide separation and capture: a review. *Journal of Environmental Sciences* 20, 14–27.
- 8) Figueroa, J.D., Fout, T., Plasynski, S., McIlvried, H., Srivastava, R.D., 2008. Advances in CO<sub>2</sub> capture technology—the U.S. Department of Energy’s Carbon Sequestration Program. *International Journal of Greenhouse Gas Control* 2, 9–20.
- 9) M.Shah, M.C. Mearthy. S.Sachdeva, A.K. Lee, H-K. Jeong, *Ind.Eng.Chem.Res.*51 (2015) 2179.
- 10) J. Eiberger, K. Wilkner, C. Reetz, D. Sebold, N. Jordan, M. de Graaff, W.A. Meulenbergh, D. Stöver, M. Bram, Influence of coal power plant exhaust gas on the structure and performance of ceramic nanostructured gas separation membranes, *International Journal of Greenhouse Gas Control*, 43 (2015) 46-56.
- 11) V.M. Aceituno Melgar, J. Kim, M.R. Othman, Zeolitic imidazolate framework membranes for gas separation: A review of synthesis methods and gas separation performance, *Journal of Industrial and Engineering Chemistry*, 28 (2015) 1-15.
- 12) Zhu, W., Hrabanek, P., Gora, L., Kapteijn, F., Moulijn, J.A., 2006. Role of adsorption in the permeation of CH<sub>4</sub> and CO<sub>2</sub> through a silicalite-1 membrane. *Industrial and Engineering Chemistry Research* 45, 767–776.